Reply to referee comments

Manuscript: ASSESSING THE PEATLAND HUMMOCK-HOLLOW CLASSIFICATION FRAMEWORK USING HIGH-RESOLUTION ELEVATION MODELS: IMPLICATIONS FOR APPROPRIATE COMPLEXITY ECOSYSTEM MODELLING

Authors: Paul A. Moore, Maxwell C. Lukenbach, Dan K. Thompson, Nick Kettridge, Gustaf Granath, and James M. Waddington

Referee: Anonymous Referee #1

Note: Our response to referee comments are in red.

General comments

Moore et al. present a methodology to classify the peatland hummock-hollow variability for carbon flux modeling using high-resolution elevation models with k-means clustering. The study has collected samples across a variety of sites and mapped the high-resolution microtopography with the structure-from-motion [sic]. This manuscript provides insights into the influence of microtopography on the uncertainties of field sampling and carbon flux modeling. Considering the importance of the peatland carbon fluxes to the global climate change, this study is relevant and necessary. Overall, this manuscript is well-written and easy to follow. However, several issues in the manuscript need to be improved before the publication. This manuscript has done a nice analysis of the DEMs and evaluated its impacts on the NPP simulation. However, the validation of the generated DEM and the model-based fluxes is weak and needs to be strengthened. Another key issue for small scale flux simulation is to identify the optimal spatial resolution for modeling. I would also suggest the authors improve the analysis to identify the optimal spatial resolution to represent the microtopography. Generally, I think that this manuscript is publishable after revisions.

We kindly thank the referee for providing comments and constructive criticisms of the manuscript. We have added validation data for SfM-derived DEMs of hummock-hollow microtopography. These data have been added to the supplemental material as a short appendix and two new supplemental figures. In regards to the small scale flux modelling, the purpose of the empirical modelling was not to represent what the actual net photosynthesis of a given plot at a given site would be, but rather to highlight the potential bias introduced by modelling microtopography as a binary system With additional analysis, we have also added modelling results which examine how flux bias is affected by information loss (i.e. smoothing of DEM). Additional details are provided in responses to specific comments below.

Specific comments

1. L20: Some key words are repeating from the title. Normally key words should be different from words in the title, as to provide additional information.

Response: We have removed duplicate words and added a new key words (structure from motion, mire).

2. Abstract: The findings on the optimal spatial resolution is quite important for the appropriate complexity of flux modeling. As mentioned in L438-439, this manuscript concluded that on the optimal

resolution to represent the spatial variability has been identified from Fig. 2 and 5. These findings should be reflected in the Abstract.

Response: We have amended the abstract to include results on the appropriate scale of complexity to measure microtopographic variability at the site and plot scale. We have also produced additional modelling results of solar insolation net photosynthesis using progressively coarse smoothing functions applied to DEMs. Smoothed results are compared to end members (i.e. model output using unsmoothed DEMs and hummock-hollow binary approach) to provide a quantitative assessment of 'appropriate' model resolution.

3. Validation of the generated elevation model is needed. The structure-from-motion technique is sensitive to the camera geometric calibration, camera position information, and the accuracy and numbers of ground control points. Validation results on the generated DEM are necessary.

Response: We had previously done an analysis of the accuracy of the SfM technique as applied to our particular measurement design. We opted to omit these results, in part, to try and keep the manuscript more concise. We are happy to include our validation results but feel that they are most appropriate to include as part of the supplemental material (see Figures 1 and 2). We have also added a couple sentences to the 'Results: Digital elevation models of microtopography' section which includes basic summary statistics of SfM accuracy from our validation measurements. The validation results included in the revised supplemental material includes both laboratory and field validation measurements. The primary purpose of laboratory measurements was to have greater accuracy and precision of x, y, z measurements. Our approach to validation was relatively simple and geared towards measurements of hummocks since the SfM approach itself has been well validated (e.g. Fonstad et al., 2013; Nouwakpo et al., 2014).

4. L237: Equations should be marked with a number. For the equation at L237, the variable x should be explained.

Response: We have added numbers to the equations and replaced 'x' in equation 2 with 'WC'.

5. L438-439: From Figure 5, it is not as easy as Figure 2 to identify the optimal resolution to represent the spatial variability. The authors can use additionally spatial analysis, e.g. semivariogram analysis, to strength these findings.

Response: We have opted to include the cumulative power spectral density in Figure 5 for consistency with Figure 2 and to provide objective information on the relative importance of scale for microtopographic variability at the plot scale.

6. The structure-from-motion can provide both DEMs and orthophotos for the study site. In the manuscript, the authors have used the DEMs for data analysis. Potentially, the orthophotos can be utilized to calculate vegetation indices to infer the vegetation growth conditions. This can improve the classification and NPP modeling. Why don't you make the best use of your data?

Response: In many cases, the actual moss species present in the plots do not match our choice of *Sphagnum* species for modelling net photosynthesis. While RGB information from SfM-derived orthophotos can certainly be used to help classify ground cover in peatlands (e.g. Harris and Baird, 2018), the purpose of the empirical modelling was not to represent what the actual net photosynthesis

of a given plot at a given site would be. Rather our purpose for using empirical models of net photosynthesis from the literature was to highlight the potential bias introduced by modelling microtopography as a binary system. Rather than focusing on inter-site species differences, the purpose of using multiple plots/sites in our analysis was primarily to include a variety of small-scale microtopographic distributions and not be biased to a particular site. Our choice of particular *Sphagnum* species to represent high-hummock, low-hummock, and hollow/lawn microtopographic classification is due to the observed niche partitioning along a microtopographic gradient presented in the literature (e.g. Andrus et al., 1983), and availability of empirical relations relating water content to water table depth, and net photosynthesis to water content in the published peer-reviewed literature.

7. Table 1: Mistakes on the Longitude. For instance, Sweden should not be -17W. I guess the fourth column should be the elevation above the mean sea level instead of the longitude.

Response: The site is located at 17 degrees longitude east, which is equivalent to -17 degrees longitude west. However, we have updated Table 1 longitudes to conform with SI standards so that positive longitude is degrees east, and negative longitude is degrees west.

8. Table 2: In Table 2, some plots have been classified into three members. However, we cannot see such three members in the histogram distribution of Figure 3 and 4. Please explain the reason.

Response: The GMM is representing the elevation distribution as a sum of Gaussian distributions. As such, a unimodal distribution that is skewed or is platy- or leptokurtic might be better represented by a multi-member Gaussian distribution than a normal distribution. While we feel that overlaying the GMM fits on Figures 3 and 4 would make them visually cluttered, we have opted to include a couple examples from our plots in the supplementary material. We have tried to include examples where the empirical distributions have clear separation in modes versus ones which don't. See Figure 3 below.

9. Figure S4. The curve should be from modeling and the dots are the measured one.

Response: Thanks for catching the error. We have updated Figure S4 accordingly.

10. Figure S8: the scale bar should be added into the spatial map. Otherwise, readers don't know the spatial scale of these maps.

Response: We have added a spatial scale to Figure S8.

11. The paper has done a nice analysis of the carbon flux modeling and assessed the impact of water table depth on the carbon fluxes. However, it is hard to evaluate whether these modeling is accurate enough or not. It would be better to add some chamber or eddy covariance measurements to validate the simulated NPP. Or at least compare the results with other relevant studies.

Response: Again, the purpose of the empirical modelling was not to represent what the actual net photosynthesis of a given plot at a given site would be, but rather to highlight the potential bias introduced by modelling microtopography as a binary system. However, we realised that it is not clear from the methods that the empirical models presented are from field-based studies of hummock-hollow plot-scale water content and flux measurements. We have revised the methods for clarity and also included the relevant source material, some of which was previously only cited in the figure captions. Moreover, we have added additional content to the discussion to compare the modelled net photosynthesis with other relevant studies.

References:

Andrus, R., Wagner, D., and Titus, J.: Vertical zonation of Sphagnum mosses along hummock-hollow gradients, Can. J. Bot., 61, 3128-3139, doi:10.1139/b83-352, 1983.

Fonstad, M. A., Dietrich, J. T., Courville, Jensen, J. L., and Carbonneau, P. E.: Topographic structure from motion: a new development in photogrammetric measurement, Earth Surface Processes and Landforms, 38(4), 421-430, doi: 10.1002/esp.3366, 2013.

Harris, A., and Baird, A. J.: Microtopographic Drivers of Vegetation Patterning in Blanket Peatlands Recovering from Erosion, Ecosystems, 1-20, doi: 10.1007/s10021-018-0321-6, 2018.

Nouwakpo, S. K., James, M. R., Weltz, M. A., Huang, C. H., Chagas, I., and Lima, L.: Evaluation of structure from motion for soil microtopography measurement, The Photogrammetric Record, 29(147), 297-316, doi: 10.1111/phor.12072, 2014.

Figures:

Figure 1: Spatial validation of structure-from-motion (SfM) method for lab (a-c) and field (d-f) microtopography. SfM reconstructions, manual measurements, and differences between the two are shown in the top, middle, and bottom panels, respectively.

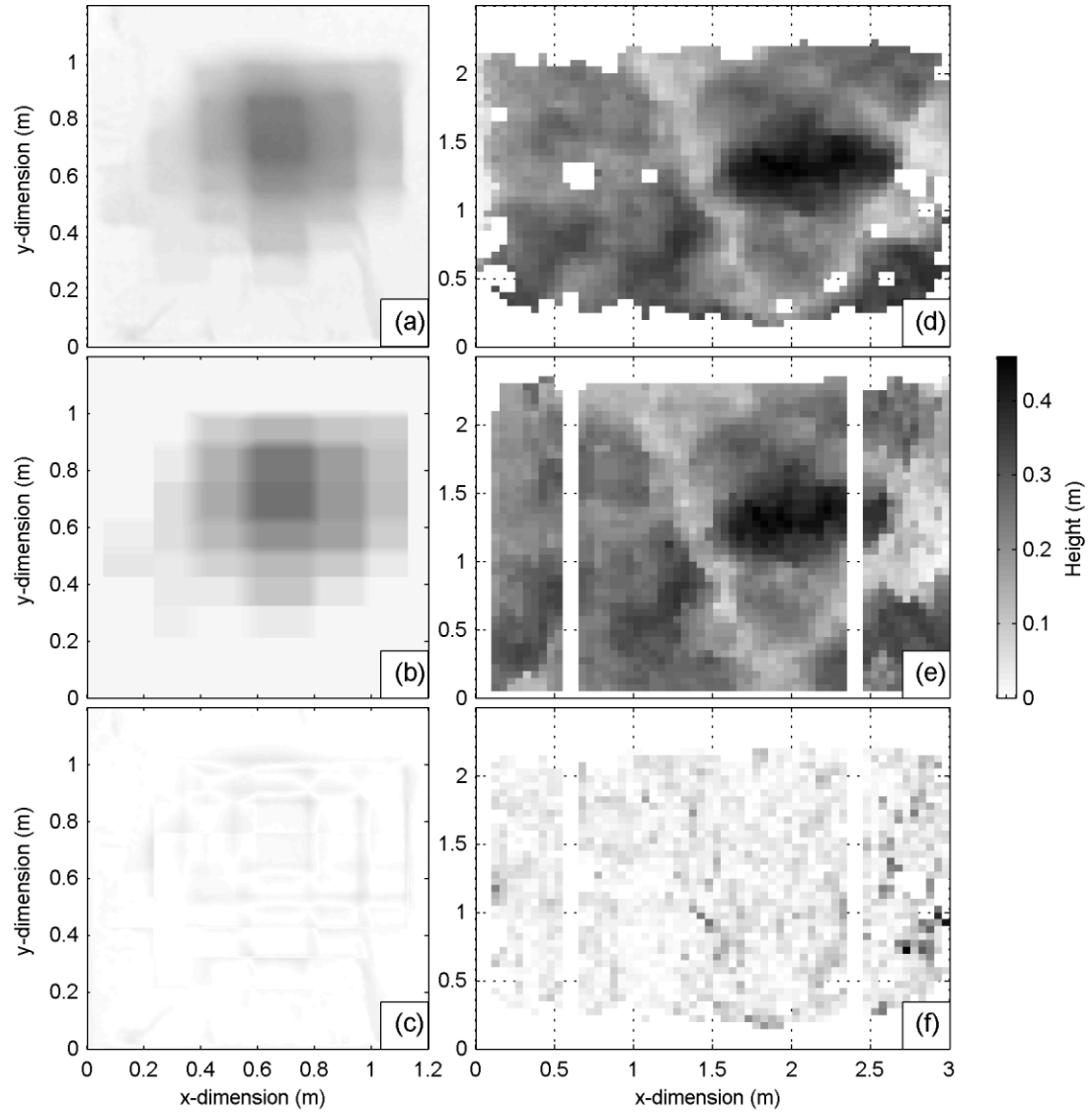

Figure 2: Distribution of residuals between structure-from-motion (SfM) reconstruction and manual elevation measurements (a). Relation between magnitude of residuals and local slope (b). Results are bin averaged, where each point is based on 150, and 1000 measurements for the field and lab tests, respectively. Error bars indicate the standard error.

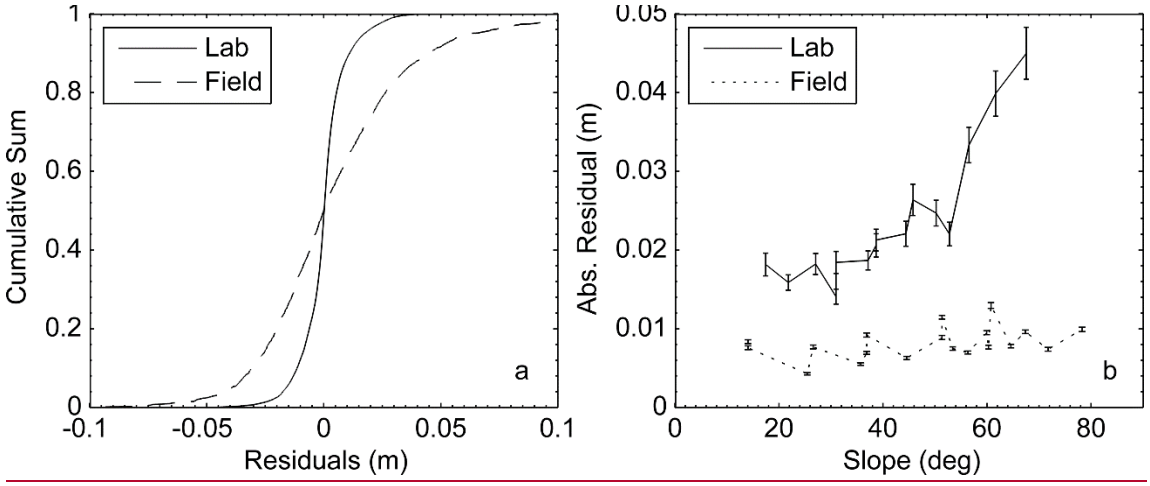

Figure 3: Gaussian mixture model (GMM) fit to relative frequency distribution of measured microtopographic elevation for four example plots. The full GMM distribution is obtained by summing the individual members. Examples for two- (upper panels) and three-member (lower panels) GMMs are given for elevation distributions which qualitatively show a separation of modes (left panels) versus ones where modes are not visually distinct (right panels).

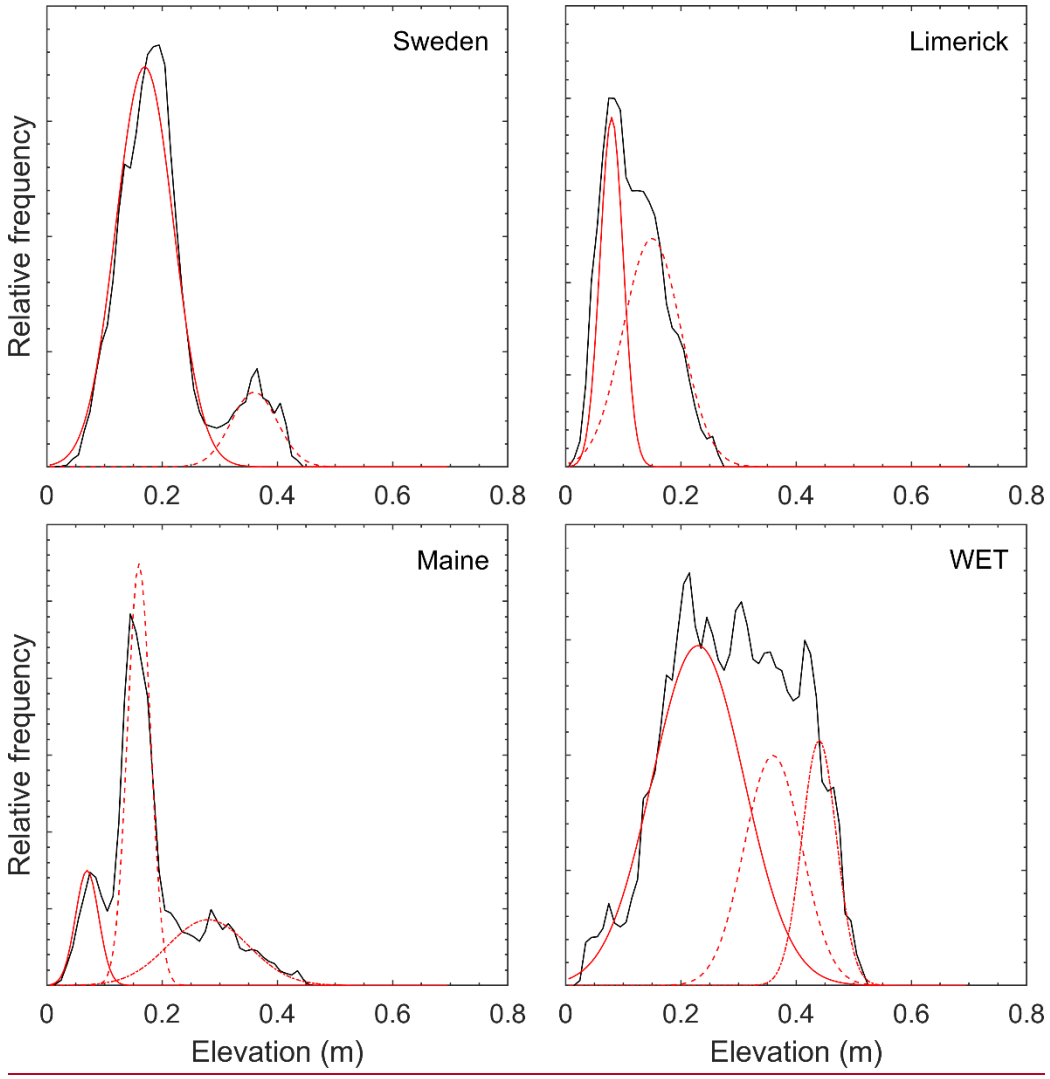

Reply to referee comments

Manuscript: ASSESSING THE PEATLAND HUMMOCK-HOLLOW CLASSIFICATION FRAMEWORK USING HIGH-RESOLUTION ELEVATION MODELS: IMPLICATIONS FOR APPROPRIATE COMPLEXITY ECOSYSTEM MODELLING

Authors: Paul A. Moore, Maxwell C. Lukenbach, Dan K. Thompson, Nick Kettridge, Gustaf Granath, and James M. Waddington

Referee: L. Kutzbach

Note: Our response to referee comments are in red.

The manuscript of Moore et al. presents a very interesting and comprehensive analysis of the microtopographic structure of boreal non-patterned bogs. The paper scrutinizes the binary hummock-or-hollow classification approach, which is often followed in sampling design or modeling of biogeochemical and ecophysiological peatland processes.

The authors applied a well-designed combination of elaborate field data acquisition methods, targeted statistical analyses and appropriate process modeling. I am particularly pleased about the creative and thorough usage of various spatial statistical methods for analyzing the heterogeneity of peatland microtopography (e.g., Gaussian mixture models, Fourier transform power spectra of microtopographic variability along transects, slope and aspect analysis for microtopographic features, fractal dimension of plots). I also like the approach of simulating water content and net primary productivity in dependence of microtopography properties as an approach to demonstrate the relevance of thorough microtopography characterization for quantification of energy and matter fluxes. The authors show that non-consideration of the full continuum of microtopographical variability can lead to serious biases in spatial averages of net primary productivity due to negligence of microforms that are intermediate between hummocks and hollows. Even more pronounced bias would be expected for, e.g., methane emissions, which are controlled by water level depth below the moss surface in a highly nonlinear way.

Thus, the presented study is of high scientific relevance and originality. However, I think that the quality of the manuscript needs to be improved. In the following, I provide lists of (1.) general comments, (2.) specific comments, and (3.) technical comments. I recommend the manuscript for publication after major revisions.

General comments

(1) The experimental design of the study needs to be better explained. It is now too difficult for the reader to find out which method was applied where. That the many analyses were conducted at various peatland sites, needs to be more clearly stated already in the introduction. Furthermore, I think that a figure explaining the study design by including maps of different scale (e.g., northern hemisphere with location of all investigated peatlands, Nobel peatland with location of random plots in detail), would help. It would be also helpful if information on site and/or spatial scale would be added to all of the figure captions.

Response: In general, we used the terms 'site-level' and 'plot-level' to systematically orient the reader in methods/results. However, it is clear from the referee's comments that improved clarity is needed. As suggested, we have explicitly included 'site-level' or 'plot-level' to figure captions where appropriate for additional clarity. It is possible that this provides the necessary additional clarity, but we have also created a figure which provides visuals of the experimental design (see Figure 1 below). Given that the main manuscript already has nine figures and the size of the new figure, we feel that the new figure is best added to the supplemental material. However, we are happy to place it in the main text as is or in a modified form if there are any strong opinions on the matter

(2) The approach for modeling water content and potential NPP needs to be better described (L. 224-240). What is the basis for the parameterizations for water content for the different microforms? Please provide references. Is NPP considered as a CO2 flux or a carbon flux? Without specifying this, the modelled NPP values cannot be checked for plausibility. However, such a plausibility check would be necessary. Please compare your modelling results with empirical data on NPP of bog microforms.

Response: The purpose of the empirical modelling was not to represent what the actual net photosynthesis of a given plot at a given site would be, but rather to highlight the potential bias introduced by modelling microtopography as a binary system. However, we realised that it is not clear from the methods that the empirical models presented are from field-based studies of hummock-hollow plot-scale water content and capitula flux measurements. We have revised the methods for clarity and also included references to the relevant source material, some of which was previously only cited in the figure captions. Moreover, we have added additional content to the discussion to compare the modelled net photosynthesis with other relevant studies.

Specific comments

L. 50: I do not like this often used comparison because it is like comparing apples with oranges: The carbon pool of peatlands is estimated over their mean peat depth (can be more than 15 m), whereas carbon pools of soils are estimated for specific reference soil depths (e.g. 1 m , 3 m). Hence, do peatlands contain one third of the upper meter of global soils or of the upper 3 m or how many meters? Furthermore, soils store not only organic carbon but also inorganic carbon!

Response: Fair enough. We have removed the comparison from the introduction.

L. 69: I would think that the area covered by a hummock can be also quite larger than 1 m2.

Response: While we agree that hummocks can be quite larger than 1 m^2, we are trying to be somewhat general in the introduction and are referring to the order of magnitude (i.e. they are far more likely to be closer to 1 m^2 than 10 m^2). Nevertheless, we have softened the language to say that hummocks typically occupy and area of up to a few square meters.

L. 96: I suggest adding the reference: Cresto Aleina F., Runkle B. R. K., Kleinen T., Kutzbach L., Schneider J., Brovkin V. (2015): Modeling micro-topographic controls on boreal peatland hydrology and methane fluxes. Biogeosciences 12: 5689-5704.

Response: We appreciate the suggestion and have added the reference.

L. 112-113: Sentence not clear to me; please rewrite! I do not understand how you want to “explore DEM-derived properties" "using multi-site plot-scale sampling".

Response: We have revised the sentence which hopefully makes it clearer now.

L. 137: Write more specific: What kind of “individuals”? Have these been scientists, students, or farmers neighboring the peatland?

Response: We replaced “individuals” with “academic peatland researchers”.

L. 157: Unit of resolution?

Response: We have updated to include the unit of resolution (i.e. pixels).

L. 234: According to SI system, do not mix units and quantities. Better “WC is the ratio of the mass of water and the mass of the non-water components of the soil (Unit: g g-1).”

Response: We have revised the sentence according to your suggestion.

L237: Specify the variable x. Probably, x equals WC, correct?

Response: Thanks for catching that. Yes, it is supposed to be WC and has been revised accordingly.

L 238: Better: “. . .represents percentage of maximum NPP”

Response: Revised accordingly.

L. 836: It is confusing to use the two terms "net photosynthesis" and "NPP" as y-axis titles of different diagrams in the same figure, respectively. Do you use the terms as synonyms? In my view, integration of net photosynthesis over time at the canopy scale leads to NPP; thus "net photosynthesis" and "NPP" would be closely related but not synonymous.

Response: We were admittedly a little sloppy with this abbreviation, where we used NPP to represent potential net photosynthesis. Understandably, this is easily confused with the widely used “net primary productivity”, so we have replaced also cases of NPP in the manuscript by either spelling out “net photosynthesis” or abbreviating as NP.

Technical comments

Response: Where relevant for the technical comments, we have revised the manuscript according to the reviewer’s comments/suggestions. Some suggestions were not adopted because the original text was removed as part of other revisions.

L. 29: Correct “examine” Done.

L. 31: Correct: “northern” Done.

L. 38: Correct: “positions” Done.

L. 50 Correct “one third”

Response: The text was removed as part of other revisions.

L. 107: Hyphenate: “plot-scale” Done.

L. 121: Hyphenate “transect-based” Done.

L. 145: I suggest writing: “ 0.1 m x 0.1 m x 0.1 m (same for similar expressions throughout the manuscript) Done.

L. 179: Comma before “and” (beginning of independent sentence) Done.

L. 186: Number the equations. Done.

L. 208: better “selected” instead of “decided” Done.

L. 239: “mo” is not a standard abbreviation for a SI unit. Please define this somewhere before using it.

Response: We have opted to simply spell it out where used.

L. 296: I would move the F statistics in parentheses to the end of the sentence. Done.

L. 311: Infelicitous usage of statistical terminology: In my view, a result can be either significant or non-significant, give a specific error probability. It cannot be strongly of weakly significant.

Response: We agree that once a level of significance is chosen, that significance is determined by whether the p-value is equal to or less than the level of significance (i.e. reject null, results are significant) or greater than the level of significance (i.e. do no reject null, results are not significant). However, we also recognize that the choice of significance level is arbitrary to some degree, and that the p-value is an indicator of probability, so that the magnitude of the p-value could be interpreted as the null hypothesis being more/less probable on a continuous scale. The use of the terminology ‘not strongly significant’ was in part an attempt to recognize greater potential type II error given the sample size and p-value near the significance level. Nevertheless, we have opted to switch the statement to ‘not significant’.

L. 374: Hyphenate: “under-samples” Done.

L. 380: Better a full stop instead of a comma after “conditions”

Response: Unfortunately, because “conditions” was used twice on line 380 of the submitted manuscript, I’m not sure which “conditions” you were referring to.

L. 465: Comma before “which” Done.

L. 507: Hyphenate “water table-dependent” Done.

L. 516: Comma before “where” Done.

L. 532: Comma before “where” Done.

Figure 1: Overview of site locations, site-level measurement design, and plot-level hummock-hollow pairs (see Table 1 for additional details).

Site locations

Red Earth Creek – site-level analysis

- *Outline of Red Earth Creek site, plot and transect locations*
- *Plot locations chosen independent of microtopography*
- *Same transect design used at Nobel site for site-level analysis.*

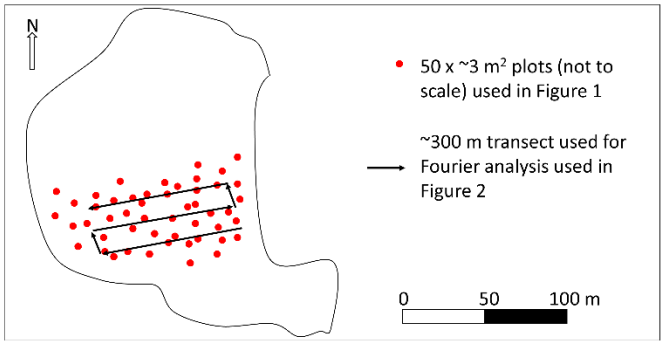

Plot-level analysis of hummock-hollow pairs:

- *Overhead view example of digital elevation model (DEM) for Seney – WET*
- *SfM-derived DEMs for qualitative and random plots form the basis for analysis presented in Figures 3–10 and all supplemental figures with the exception of Figure S5*

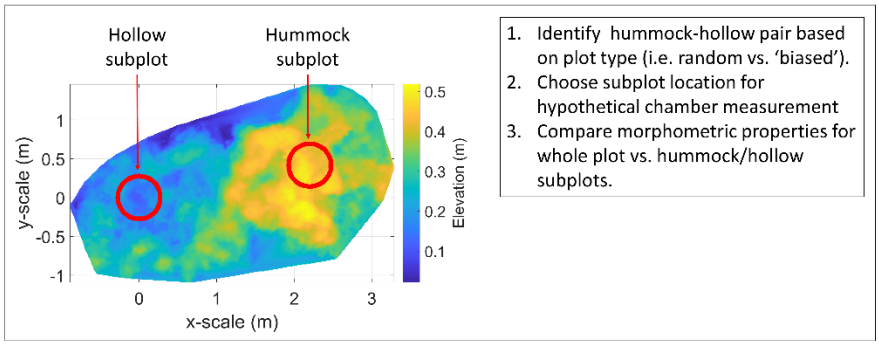

ASSESSING THE PEATLAND HUMMOCK-HOLLOW CLASSIFICATION FRAMEWORK USING HIGH-RESOLUTION ELEVATION MODELS: IMPLICATIONS FOR APPROPRIATE COMPLEXITY ECOSYSTEM MODELLING

Paul A. Moore[1*], Maxwell C. Lukenbach[1], Dan K. Thompson[2], Nick Kettridge[3], Gustaf Granath[4], and James M. Waddington[1]

[1] School of Geography and Earth Sciences, McMaster University,1280 Main Street West, Hamilton, ON, L8S 4K1, Canada

[2] Northern Forestry Centre, Canadian Forest Service, Natural Resources Canada, Edmonton, Alberta, AB, T6H 3S5, Canada

[3] School of Geography, Earth and Environmental Sciences, University of Birmingham, Edgbaston, Birmingham, B15 2TT, United Kingdom.

[4] Department of Ecology and Genetics, Uppsala University, Norbyvägen 18D, 736 52 Uppsala, Sweden

* Corresponding author: Paul Moore (paul.moore82@gmail.com)

Manuscript for submission to Biogeosciences

KEY WORDS: microtopography, morphometry, sampling design, structure from motion, mire

Deleted: peatland,

Deleted: hummock, hollow,

Deleted: ecosystem modelling, digital elevation model

ABSTRACT

The hummock-hollow classification framework used to categorize peatland ecosystem microtopography is pervasive throughout peatland experimental designs and current peatland ecosystem modelling approaches. However, identifying what constitutes a representative hummock-hollow pair within a site and characterizing hummock-hollow variability within or between peatlands remains largely unassessed. Using structure-from-motion (SfM), high resolution digital elevation models (DEM) of hummock-hollow microtopography were used to: 1) examine how much area needs to be sampled to characterize site-level microtopographic variation; and 2) examine the potential role of microtopographic shape/structure on biogeochemical fluxes using plot-level data from 9 northern peatlands. To capture 95% of site-level microtopographic variability, on average an aggregate sampling area of 32 m^2 composed of ten randomly located plots was required. Both site- (*i.e.* transect data) and plot-level (*i.e.* SfM-derived DEM) results show that microtopographic variability can be described as a fractal at the sub-metre scale, where contributions to total variance are very small below ~0.5 m length scale. Microtopography at the plot-level was often found to be non-bimodal, as assessed using a Gaussian mixture model (GMM). Our findings suggest that the non-bimodal distribution of microtopography at the plot-level may result in an under-sampling of intermediate topographic positions. Extended to the modelling domain, an under-representation of intermediate microtopographic positions is shown to lead to potentially large flux biases over a wide range of water table positions for ecosystem processes which are non-linearly related to water and energy availability at the moss surface. Moreover, our simple modelling results suggest that much of the bias can be eliminated

Deleted: d

Deleted: with vegetation removed

Formatted: Font: Italic

Formatted: Font: Italic

Deleted: We further present non-destructive transect-based results as an alternative to the SfM approach.

by representing microtopography with several classes rather than the traditional two (*i.e.* hummock/hollow). A range of tools examined herein can be used to easily parameterize peatland models, from GMMs used as simple transfer functions, to spatially explicit fractal landscapes based on simple power law relations between microtopographic variability and scale.

INTRODUCTION

Northern peatlands in the maritime-temperate, boreal, and subarctic have been persistent terrestrial sinks for carbon throughout the Holocene, storing on the order of 500 Gt of carbon as organic soil deposits (Yu, 2012). However, these peatland carbon stores are now considered to be at risk from the effects of climate change due to warmer temperatures and prolonged periods of drought which would increase carbon loss through decomposition and increased wildfire consumption (Moore et al., 1998; Yu et al., 2009; Turetsky et al., 2002; Kettridge et al., 2015). While these positive feedbacks cause carbon loss (*e.g.* Ise et al., 2008; Blodau et al., 2004), the long-term stability of peatland carbon may be maintained by negative ecohydrological feedbacks that promote resilience to environmental change (Belyea and Clymo, 2001; Waddington et al., 2015; Hodgkins et al., 2018). These negative feedbacks depend, in part, on the presence of microtopography (microforms) that provides spatial diversity in ecohydrological structure and biogeochemical function across a peatland (Belyea and Clymo, 2001; Belyea and Malmer, 2004; Eppinga et al., 2008; Pedrotti et al., 2014; Malhotra et al., 2016).

Formatted: Font: Italic

Deleted: approximately one-third of all global

Deleted: carbon

Peatland microform classification is typically defined by their proximity to the water table and characteristic vegetation assemblages, such as different species of *Sphagnum* moss and cover of woody shrubs (Andrus et al., 1983; Rydin and McDonald, 1985; Belyea and Clymo, 1998). Hummocks and hollows occur at a spatial scale of 1 to 10 m (S2 – Belyea and Baird, 2006), with hummocks typically covering an area of up to a few square metres. The hummock surface is typically located ~0.20 m or higher above the water table (Belyea and Clymo 1998; Malhotra et al., 2016). Hollows are closer to the water table and may occasionally be inundated, and 'lawns' are intermediate to hummocks and hollows (Belyea and Clymo, 1998).

Deleted: the surface of
Deleted: usually
Deleted: n
Deleted: the order of
Deleted: 1
Deleted: m^2

Conceptualizing and qualitatively classifying complex peatland microtopography as hummocks and hollows is common in peatland research (*e.g.* Waddington and Roulet 1996; Belyea and Clymo 2001; Nungesser 2003; Benscoter et al., 2005; Bruland and Richardson 2005; Moser et al., 2007) as it is simple and allows for straightforward sampling designs, however, the visual characterization of hummocks and hollows is subjective and has the potential to produce biased results for several reasons. First, although microform vegetation and hydrology may be included in detailed study site/method descriptions, these characteristics may be quite different for microforms classified as hummocks at one study site compared to hummocks at a different study site. Biogeochemical function (ecosystem fluxes) may differ for microforms within a site (*e.g.* Bubier et al., 1993; Pelletier et al., 2011), but if the vegetation and hydrology of those microforms vary for different peatlands, assumptions for hummock and hollow biogeochemical function at one site may not be applicable to other peatlands. Given

that there may also be large differences in the relative/absolute height and surface roughness of microforms between sites, comparing studies with hummock and hollow microforms as a central component of the sampling design can be problematic. Moreover, the surface area, spatial distribution, and relative proportion of hummock and hollow microforms present within a peatland also vary between sites (*e.g.* Moore et al., 2015), which may introduce bias into sampling design. For example, researchers may over-sample the visually obvious extremes of the hummock-hollow continuum. Given that several peatland hydrological and ecosystem carbon models parameterize peat decomposition, production and hydraulic properties based on peatland microform classification (*e.g.* Cresto Aleina et al., 2015; Dimitrov et al., 2010; Sonnentag et al., 2008), the aforementioned sampling and classification biases may also lead to issues in determining the scale and complexity required for ecosystem modelling (*e.g.* Larsen et al., 2016).

The construction of a digital elevation model (DEM) in a peatland allows for the classification of microforms based on quantitative measures (*e.g.* relative position, slope, roughness) (*e.g.* Mercer and Westbrook, 2016; Rahman et al., 2017) rather than relying on qualitative/visual methods. Given the wide use and adoption of the hummock-hollow conceptual framework, we examine the potential utility of DEM quantitative techniques to overcome the concerns with the dominant qualitative hummock and hollow framework/classification scheme. As such, the two main objectives of this study were to: (i) provide a geostatistical/geospatial description of microtopographic variation in peatlands; and (ii) to use simple physically-based and empirical models to examine the

Deleted: or

Deleted: plot scale

effect of measured microtopographic complexity on ecosystem fluxes. For the first objective, our two main focuses were: i) using a case-study approach, assess how much area needs to be sampled at a given site in order to be able to adequately quantify microtopographic variability within an unpatterned peatland; and ii) using hummock-hollow plots across multiple peatlands, quantify morphometric properties (*e.g.* microtopography height distribution, slope, and roughness) derived from high-resolution surface DEMs, which may be useful as microtopographic metrics.

Deleted: multi-site

Deleted: plot-scale sampling

Deleted: explore

Deleted: DEM-derived

Deleted: of peatland microforms

METHODS

Experimental design

We first evaluated how much sampling area is needed to capture the overall microtopographic variation of an unpatterned site using both structure-from-motion (SfM) (see Brown and Lowe 2005; Mercer and Westbrook 2016) and a transect-based sampling approach (Figure S1 – middle panel). To accomplish this, we randomly sampled 50 plots for SfM reconstruction in a peatland near Red Earth Creek, AB (56.54°N 115.22°W) (hereafter referred to as site-level). In addition, we manually measured surface elevation along several 50 m transects at 0.05 m intervals covering the plot area at the Red Earth Creek site. Secondly, we used SfM to examine morphometric properties at the plot scale in 9 boreal/hemi-boreal, non-permafrost, peatlands (4 in Canada, 4 in USA, 1 in Sweden; see Table 1 and Figure S1 – top panel) using two different approaches. The first approach involved randomly selecting 9 plot locations within a single site and creating a plot around the random location which was perceived to contain a hummock-hollow pair. The second approach involved

Deleted:

Deleted: ombrotrophic

qualitatively choosing what was perceived to be a representative hummock-hollow pair at 9 different sites. The aim of our approach was to highlight the potential breadth of variation in morphometric properties which might be observed either within a site (*i.e.* implications for small sample size) or across sites (*i.e.* highlight potential challenges with site inter-comparisons without supporting information of peatland microtopographic metrics). For both randomly located plots and qualitatively chosen plots, academic peatlands researchers were asked to identify a central point for a hummock and hollow subplot within the larger microtopography plot.

Deleted: individuals

Site preparation and image acquisition protocol

All vascular vegetation was removed from the plot area using scissors and hand pruners in order to provide an unobstructed view of the surface microtopographic variation (moss surface) for imaging. Matte-colored discs (n=20) of 0.04 m diameter were placed randomly on the clipped surface to provide reference points for better correlation between images. To provide absolute scale and orientation, two boxes of known dimensions (0.1 m × 0.1 m × 0.1 m) were placed in each plot and levelled prior to image acquisition. Images of each target area were taken via at least two circuits around the plot, with images taken from two separate vertical viewing angles (see http://www.cs.cmu.edu/~reconstruction/basic_workflow.html for third party description of general workflow). Distance to target area was set so that a large portion of the clipped area was visible in each image. To produce different horizontal viewing angles, images were taken every one or two paces around the perimeter of the plot. This procedure yielded 41 to 282 overlapping images from multiple view-points of the plot areas, which ranged in size from 3.2 to 10.1 m^2 (Table 1). Images were taken during either clear-sky

or over-cast conditions near mid-day during the summer to avoid changing lighting conditions and to limit self-shadowing of the surface. Images were captured with digital cameras using automatic exposure settings. Prior to analysis, all images were downscaled where necessary to a common resolution of 2048 x 1536 pixels using a Lanczos3 filter.

Digital elevation models of microtopography

A point-cloud of the moss surface was generated using an SfM approach (Brown and Lowe 2005; Mercer and Westbrook 2016) using the program Visual SfM (Wu, 2011). Visual SfM identifies image features for cross-comparison using a scale-invariant feature transform (Lowe, 1999), and then matches features between images in a pairwise manner. Effectively, this creates multiple stereo-pairs from which camera position and scene geometry can be estimated through triangulation. This procedure yielded average point cloud densities ranging from 3-59 pixels cm^{-2} for the imaged plots (Table 1).

Prior to generating the DEMs, point clouds were cropped to the region of interest (*i.e.* area of clipped vegetation), then scaled, levelled, and oriented using the rendered reference objects. DEMs were produced using the MATLAB function *TriScatteredInterp* (MATLAB R2010a, The Mathworks), which performs Delaunay triangulation of the point clouds. DEMs were generated on a 0.01 m x 0.01 m grid using natural neighbor (Voronoi) interpolation. The DEMs were smoothed using a mean filter window with a size of 0.03 m x 0.03 m. Finally, a mask was applied to the DEMs to remove reference

objects. The accuracy of the method was assessed (see supplemental Appendix 1 and corresponding Figures S2 and S3) yielding root mean square error values less than 0.01 m in the x, y, z under laboratory conditions. Median absolute deviation of elevation between the DEM and lab and field validation plots was 0.004 m and 0.018 m, respectively.

Capturing site-level microtopographic variation

Plots from the Red Earth Creek peatland were ~3.5 m^2, and differences between plot elevation for the 50 plots were surveyed using a Smart Leveler digital water level (accuracy ±2.5 mm), with offsets applied to DEMs. A Monte Carlo re-sampling approach was used to evaluate how total variance in microtopographic elevation increased with increasing sample size. For each sample size (*i.e.* 1-50), 200 random re-samplings were performed. To estimate the change in variance with increasing sample size, a rectangular hyperbola was fit to the mean variance (y) versus sample size (x):

$$y = \frac{ax+b-\sqrt{(ax+b)^2-4axbc}}{2c} \quad (1)$$

where *b* is the estimated maximum total variance, and *a* and *c* are initial slope and concavity parameters.

To evaluate the dominant scale of microtopographic variation which contributes to total variance, a fast Fourier transform (*fft* function in MATLAB) was used to estimate the power spectral density (PSD) of microtopographic variation along an artificially constructed 300 m long transect (combination of multiple transects). Manual measurements of moss surface elevation were taken every 0.05 m along multiple

Deleted: six 50 m

connected transects at the Red Earth Creek, AB and Nobel, ON site using the Smart Leveler.

Plot-level microtopographic variation

Plot-level microtopographic variation was analyzed using randomly and qualitatively chosen plot locations listed in Table 1. Based on the hummock-hollow conceptual model, our *a priori* assumption was that a hummock-hollow pair would have a bi-modal distribution of surface elevation. Our null hypothesis was that microtopography would follow a bi-modal distribution, so we evaluated DEM height distributions using 1– to 3–member Gaussian mixture models (GMM) to evaluate whether 2-member GMMs would best explain height distributions. GMMs were fit to DEM height distributions using the MATLAB function *gmmdistribution.fit*, which uses an iterative expectation maximization algorithm to determine GMM parameters representing maximum likelihood estimates. The GMM fit function was seeded with initial parameter estimates using *k*–means cluster analysis. The best model was selected based on the minimum Akaike information criteria (AIC).

Deleted: decided

Surface slope and aspect were evaluated using the computed surface normals for each point and eight connected neighbours of the DEM. The fractal dimension of plots was evaluated using radially averaged PSD derived from an *fft* of elevation data. The Hurst (*H*) exponent (values of 0–1) presented herein is related to fractal dimension as 3-*H*, where the slope of the PSD curve in log space is -2(H+1).

Modelled moss surface insolation and productivity at the plot-level

Potential moss surface insolation was modelled using the formulation presented in Kumar et al. (1997) to account for earth-sun geometry, surface slope and aspect, and diffuse radiation under clear-sky conditions. Total potential insolation was evaluated on an annual basis and normalized relative to total insolation on a flat surface for each plot location.

For moss net photosynthesis (NP) and capitula water content (*WC*), each plot was classified into three units based on relative elevation which notionally correspond with hollow/lawn, low hummock, high hummock. K-means clustering was used to perform unsupervised classification of microtopographic elevation (Figure S4). A separate parameterization for moss NP and WC was used for each elevation cluster. Parameterizations for hollow/lawn, low hummock, and high hummock were obtained from *Sphagnum* species of the section Cuspidata, Sphagnum, and Acutifolia, respectively (Figure S5). Empirical relations between WC and water table depth (WTD) were derived from Strack and Price (2009) and Rydin (1985), and were modelled as follows:

$$WC = p_1 \cdot \ln(p_2 \cdot WTD) + p_3 \quad (2)$$

where WC is the ratio of the mass of water to the sample dry weight (g g^{-1}), and $p_{1\text{-}3}$ are fitted parameters. WC was restricted to a range of 1–25 g g^{-1}. A rational function was used to model the relation between moss capitula NP and WC according to the results in Schipperges and Rydin (1998), where:

$$NP_{pot} = 100 \cdot \left(\frac{p_4 \cdot WC^2 + p_5 \cdot WC + p_6}{WC^2 + p_7 \cdot WC + p_8}\right) \cdot NP_{max}^{-1} \quad (3)$$

Deleted: primary productivity
Deleted: P
Deleted: 1
Deleted: P
Deleted: 2
Deleted: An e
Deleted: was
Formatted: Tab stops: 16.51 cm, Right
Deleted: in
Deleted: water
Deleted: dry weight
Formatted: Not Superscript/ Subscript
Deleted: water
Deleted: dry weiight
Deleted: P
Formatted: Tab stops: 16.51 cm, Right
Deleted: P
Deleted: x
Deleted: x
Deleted: x
Deleted: P

where NP_{pot} represents percentage of maximum NP, and $p_{4\text{-}8}$ are fitted parameters. Estimates of 2.7, 5.6, and 6.5 g m^{-2} day^{-1} for NP_{max} were used to represent *Sphagnum* species of section Cuspidata, Sphagnum, and Acutifolia, respectively (Nungesser, 2003).

Deleted: P
Deleted: %
Deleted: P
Deleted: 83
Deleted: 170
Deleted: 198
Deleted: mo
Deleted: P

RESULTS

Site-level microtopographic variation

In characterizing microtopographic variability across the Red Earth Creek site (Figure S1 – middle panel), our data shows that variability in surface elevation increases asymptotically with sample size (*i.e.* area sampled) and is well predicted by a rectangular hyperbola (r^2=0.98; p<<0.01) (Figure 1). Based on the asymptote of the fitted rectangular hyperbola (0.147 m), Figure 1 shows that on average an area of 32 m^2 (*i.e.* 9 random plots of ~3.5 m^2 size) contains roughly 95% of the predicted site-scale microtopographic variability. Even though increasing the number of plots by a factor of 5 (*i.e.* ~50 plots) has little effect on the average variance in surface elevation, the range associated with re-sampling is reduced by about half (Figure 1 – shaded area).

Deleted: .
Deleted: .

While the Red Earth Creek multi-plot DEM data provides the ability to assess the area required to capture site-scale microtopographic variability for a small unpatterned Alberta peatland, it does not directly provide information on what spatial scales contribute most to overall variability. The power spectral density (PSD) of manual elevation transects from both the Red Earth Creek and Nobel sites suggests that most

of the microtopographic variation for these two surveyed sites occurs at spatial scales between 1–10 m (Figure 2 – cumulative curves). Both sites have qualitatively similar PSD curves in log-space with a roll-off at spatial scales between 2.4–2.9 m (break point of piecewise regression). Moreover, the PSD of microtopographic variation appears to be well described by a power law (*i.e.* relatively smooth slope in log space despite noise) at small spatial scales resulting in a Hurst exponent (see Methods for relation to fractal dimension) between 0.14–0.26. For both transects, 95% of total variance is captured at a length scale greater than ~0.6 m

Plot-level hypsometry and fractal dimension

There is a characteristic difference in the elevation distribution of whole-plots compared to that of the corresponding hummock-hollow subplots for both qualitatively (Figure 3) and randomly (Figure 4) chosen plot locations. The elevation distributions for hummock-hollow subplots tend to have a clear separation of modes (Figures 3-4 B-panels). The degree of separation in modes has a moderately weak correlation (r^2 = 0.31) but significant linear relation (F_{16} = 7.1, p = 0.017) with the interquartile range in elevation of the whole plot. On average, the elevation range absent from the hummock-hollow subplots represents roughly 31% of the microtopographic range of the whole plot. When all hummock-hollow subplots are aggregated across randomly selected plots (*i.e.* Nobel, ON site), the whole elevation distribution is captured (Figure S6). However, there remains a bias towards higher elevations being sampled in the aggregated subplot elevation distribution compared to the aggregated whole plot elevation distribution.

Deleted: .
Deleted: 6
Deleted: 3.1
Deleted: 61
Deleted: 79
Deleted: .
Deleted: .
Deleted: .
Deleted: microtopographic
Deleted: in
Deleted: 25
Deleted: .
Deleted: 3

In testing the null hypothesis of bimodally distributed relative surface elevation at the plot scale, we examined the goodness of fit of one-, two-, and three-member GMMs (see Figure S7 for example GMM fits). An assessment of all 18 plots suggests that two- or three-member GMMs tend to provide a better fit to reconstructed elevation distributions compared to a one-member (*i.e.* normal) distribution. Based on AIC values, the one-member GMM was best for only 3 plots, while two- and three-member GMMs were best for 6 and 9 plots, respectively (Table 2). In contrast, when GMMs were fit to hummock-hollow subplot data, the two-member GMM tended to outperform one- and three-member GMMs.

The mean (μ) and standard deviation of elevation for hummock and hollow subplots were grouped and compared according to plot selection method (*i.e.* random within site versus qualitative between site selection). Since the μ parameter corresponds with relative elevation, we took the difference between the two members (*i.e.* μ_{hum}–μ_{hol}) for comparison purposes. Overall, the qualitatively chosen plots appear to have similar relative hummock heights (μ_{hum}–μ_{hol}) (0.21±0.08 m) compared to the randomly chosen plots. (0.19±0.09 m) ($F_{1,16}$=0.2; p=0.66). Variation in elevation tended to be higher in hummock subplots (0.031±0.012 m) compared to hollow subplots (0.021±0.008 m) (microform; $F_{1,32}$=9.3, p=0.005), where the difference between hummock and hollow subplots was similar when comparing qualitatively and randomly chosen sites (microform × plot type; $F_{1,32}$=0.05; p=0.82).

Deleted: ($F_{1,16}$=0.2; p=0.68)

Deleted: lower

Deleted: hollow

Deleted: 2

Deleted: hummock

Deleted: 2

Deleted: 9

Deleted: 0

Deleted: 2

Deleted: 9

Depending on the underlying structure of spatial variability, surface roughness can be

highly dependent on the scale of analysis. A two-dimensional power spectral density of elevation provides a means to formally describe the change in roughness with scale (Figure. 5). The power spectral density of elevation was found to be a linear function of length-scale across the 0.05–1 m range in log–log space (r^2_{adj}>0.97) and is the basis for the Hurst exponent (*H*) (see methods for relation to fractal dimension). While the distribution of *H* for qualitatively chosen plots (0.70±0.18) was higher compared to randomly chosen plots (0.58±0.10) (*i.e.* comparatively less 'complexity' at finer spatial scales), the difference was not significant ($F_{1,16}$ = 3.06; p = 0.10). Similar to the transect-based analysis (see *Site-level microtopographic variation* section), 95% of total variance is captured at a length scale greater than 0.37-0.90 m.

Plot-level slope, aspect and solar insolation

A Weibull distribution provided a good fit to the slopes for the reconstructed DEMs (Figure S8), where the average, maximum, and minimum RMSE were 0.10%, 0.14%, and 0.06%, respectively, based on a relative frequency distribution with 1° bin sizes. When grouped according to qualitatively versus randomly chosen plots (Table 1), the modal slope for whole plots was 18.6±4.5° and 20.0±4.8°, respectively. Similarly, the distribution of standard deviation in slope for qualitatively and randomly chosen plots was 13.1±1.5° and 12.9±2.0°, respectively. Comparing the parameter distributions from the Weibull fit for qualitatively and randomly chosen plots, it was found that there was no significant difference in the mean scale (analogous to mode) and shape (analogous to standard deviation) parameters (scale: p=0.72, $F_{1,16}$=0.13; shape: p=0.24, $F_{1,16}$=1.47).

Deleted: 96
Deleted: 3
Deleted: 60
Deleted: 1
Deleted: strongly
Deleted: 3
Deleted: 075
Formatted: Font: Italic
Deleted: .
Deleted: 4
Deleted: 21.5
Deleted: 4
Deleted: 23.4
Deleted: 5.7
Deleted: randomly
Deleted: qualitatively
Deleted: 4.6
Deleted: 3
Deleted: 4.5
Deleted: 1
Deleted: 44
Deleted: 62
Deleted: 88
Deleted: 0.02

While modal slope tended to only be slightly higher in the hummock subplots (20.3±6.9°) versus hollow subplots (16.0±5.1°), there was greater distinction in the prevalence of steep slopes (*i.e.* >45°) in hummock subplots (8.7±8.6%) versus hollow subplots (3.4±5.4%) (Figure S9). Comparing slope in the hummock/hollow subplots to the 3-member GMM clusters (high, intermediate, and low elevations – for example see Figure S4), we see that the subplots tend to be somewhat flatter compared to the rest of the plot, particularly for hollow subplots (Figure S9).

Figure 7 shows how slope and aspect of the Seney WET plot affect potential solar insolation at the moss surface under ideal conditions (i.e. clear-sky, sparse vegetation), where broadly similar results are obtained for all plots (Figure S10). Potential solar insolation is significantly affected by aspect ($F_{7,24984}$ ≥ 543.9, p<<0.01) (e.g. Figure 7a) and its interaction with slope ($F_{7,45606}$ ≥ 3579.4, p<<0.01) (e.g. Figure 7b) across all plots, where on average, south facing slopes receive double the potential solar insolation compared to north facing slopes. Based on measured slope and aspect at randomly and qualitatively chosen plots, median potential solar insolation for a south-facing slope is 14-25% greater compared to a flat surface. Similarly, for a north-facing slope, median potential solar insolation is 21-45% lower (Figure S10).

Plot-level empirical model of moss productivity using high resolution DEMs

Assuming a flat water table at the plot-level, Figure 8 shows how modelled NP_{pot} varies with WTD relative to the average hollow surface. Hollows tend to have a comparatively

Deleted: 2.9
Deleted: 8
Deleted: 9.5
Deleted: 6
Deleted: 0
Deleted: 14.8
Deleted: 10.4
Deleted: 8.4
Deleted: 9.5
Deleted: .
Deleted: 5
Deleted: .
Deleted: 1
Deleted: .
Deleted: S5
Deleted: 60820
Deleted: 290.8
Deleted: 7043.7
Deleted: aspect
Deleted: 2
Deleted: 4
Deleted: aspect
Deleted: 18
Deleted: 0
Deleted: 6
Deleted: P

narrow range of WTD (*i.e.* 0–0.15 m) over which the moss is expected to be highly productive compared to hummocks. Despite using species-dependent NP_{pot}-WC relations, the large differences in water table range over which hummock and hollow NP_{pot} is high is largely driven by the WC-WTD relations (Figure S5). Where moss species have large differences in NP_{max} and different characteristic water retention, NP_{pot} rarely overlaps between microtopographic classes (Figure 8). If we ignore the effect of species-dependent characteristics (i.e. NP_{max}, NP_{pot}–WC, and WC–WTD) and use a single parameterization (herein low-hummock), differences between microtopographic classes tend to be smaller for shallow water table conditions (Figure S11), yet there remains a characteristic difference in mean NP_{pot} between microtopographic classes.

From a scaling perspective, modelled NP_{pot} (Figures 8 and S11) was used to compare spatially explicit estimates with averages based on the notional chamber subplot (i.e. pre-determined 0.37 m^2 area in perceived hummock and hollow — see methods and Figure S1, lower panel). In general, spatially explicit NP_{pot} estimates tended to be higher/lower than the scaled hummock-hollow subplot estimates depending on whether the water table was relatively shallow/deep (Figure 9a). The maximum positive bias between the spatially explicit and scaled hummock–hollow subplot NP_{pot} values ranged from 0.52–1.37 g m^{-2} day^{-1} under shallow water table conditions, while the negative bias ranged from -0.22 to -1.98 g m^{-2} day^{-1} under deeper water table conditions. Using a single parameterization for NP_{pot} tends to result more consistently in positive bias between the spatially explicit and scaled hummock-hollow subplot models (Figure 9b),

Formatted: Font: Italic
Deleted: P
Deleted: P
Deleted: 2
Deleted: P
Deleted: P
Deleted: P
Deleted: P
Deleted: average
Deleted: 7
Deleted: P
Deleted: P
Deleted: S7
Deleted: were
Deleted: plot
Deleted: P
Deleted: P
Deleted: 21.1
Deleted: 40.1
Deleted: mo
Deleted: 5.9
Deleted: 40.9
Deleted: mo
Deleted: average
Deleted: P
Deleted: overwhelmingly

where maximum bias is up to 1.98 g m^{-2} day^{-1}. Averaged across all 18 plots, the location of the subjective hummock subplot broadly overlapped with the k-means high-hummock classification (94%), with only small portions overlapping with the low-hummock classification (6%). Similarly, the location of the subjective hollow subplot broadly overlapped with the k-means hollow/lawn classification (79%), with only small portions overlapping with the low-hummock classification (20%). In this study, our results indicate that the subjective choice of hummock and hollow subplot location (e.g. for chamber flux measurement) systematically under-samples intermediate topographic positions. For the NP_{pot} model using separate parameterization for the microtopography classes, the low-hummock class tends to remain distinct from both the hollow/lawn and high-hummock class except under very dry conditions (see Figure S12 for an example). For the uniform parameterization, the low-hummock classification is distinct from the other two classes only under wet conditions. In contrast, the low-hummock classification behaves like the hollow/lawn under moderately dry conditions, and behaves like a high-hummock under very dry conditions.

Evaluated over a large range of WTD (*i.e.* 0–0.6 m below average hollow surface), the root mean square difference (RMSD) between NP_{pot} (as % of maximum) calculated using the SfM-derived DEMs and binary classification using the average hummock and hollow subplot elevation was 20±6%. However, bias between the DEM-based NP_{pot} and subjective hummock/hollow elevations is greatly reduced if an unbiased binary classification is used. The RMSD when hummock and hollow elevations are set to the 66^{th} and 33^{rd} percentile of measured elevation distribution is reduced to 5±2% (Figure

Deleted: ranges from 22.7

Deleted: 58.9

Deleted: mo

Deleted:

Deleted: This is exemplified in Figure S8 which shows the spatial distribution of NPP_{pot} for one of the plots.

Deleted: P

Deleted: s

Deleted: ,

Formatted: Font: Italic

Formatted: Superscript

Formatted: Superscript

10). Moreover, bias is largely eliminated with the use of only several elevation classes where, for example, an RMSD of 1% or less is achieved using 2-7 elevation classes.

DISCUSSION

Assessing microform representativeness

In studies which use the hummock-hollow microtopography classification as part of their sampling design, there are many cases in which the plot choice is said to be representative (*e.g.* Kettridge and Baird 2008; Laing et al., 2008; Nijp et al., 2014), but often lacks detail on how representativeness was assessed. For example, when characterizing the surface within an eddy covariance flux measurement footprint, it is common to only sample one or few hummock-hollow pair(s) (*e.g.* Lafleur et al., 2003; Humphreys et al., 2006; Peichl et al., 2014; Moore et al., 2015). Similarly, for direct measurements of surface fluxes where microtopography is considered explicitly, chamber-based measurements typically use between four and eight replicates (*e.g.* Frenzel and Karofeld 2000; Turetsky et al., 2002; Forbrich et al., 2011; Petrone et al., 2011) per microtopographic unit. For peatland studies which use random plots, as many as 30 plots per site have been reported (*i.e.* Wieder et al., 2009), yet earlier studies have reported using as few as one to four plots to characterize a site (*e.g.* Crill et al., 1988; Shannon and White 1994; Regina et al., 1996). Using the Red Earth Creek results as a reference, for studies which have 4-8 replicates, 2-3 microtopographic units (*e.g.* hummock, lawn, hollow), and the more common chamber size of roughly 0.6 m x 0.6 m, we would infer from our results that the typical total sample area for chamber flux

measurements in a peatland ecosystem would capture on the order of 70-86% of site-scale microtopographic variability in their plots. It should be noted however that the simple assessment above assumes that chamber placement is random. In cases with lower replication of two microtopographic units, our results suggest that the uncertainty associated with repeated sampling is relatively high (Figure 1 – shaded area) and that the choice of two microtopographic units could lead to an under-sampling of intermediate topographic positions (*e.g.* Figures 3-4 B-panels). When the ecosystem processes of interest are not measured across the range of variability observed at the site-scale, particularly for non-linear processes, then scaling from process-based, or simply plot-scale measurements, is at risk of being biased. Our simple empirical model of moss NP_{pot} demonstrates that flux bias can be large relative to NP_{max} and is strongly dependent on water table depth (Figure 9). While water table is a first order control on peat water content (Hayward and Clymo, 1982), moss capitula water content, however, has been shown to be less sensitive to water table (Strack and Price, 2009). Moreover, the sensitivity of *Sphagnum* CO_2 assimilation to water level has been shown to be strongly dependent on precipitation (Robroek et al., 2008). Using the simple empirical model and measured WTD at the Seney site (see Moore et al., 2015), the magnitude of modelled NP_{pot} (seasonal average of 1.2–3.8 g m^{-2} d^{-1}) is less than seasonal average chamber-measured GPP values (see Ballantyne et al., 2014), though the later includes vascular vegetation. Nevertheless, the empirical NP-modelled values are broadly consistent with field measured *Sphagnum* production (e.g. Moore, 1988; Waddington et al., 2003). Although NP_{pot} estimates are strongly influenced by the parameterization used (*e.g.* Figure 8 and S11), there remains a large bias between the spatially explicit

Deleted: .
Deleted: .
Deleted: P
Deleted: P
Formatted: Font: Italic
Formatted: Subscript
Formatted: Superscript
Formatted: Font: Italic
Deleted: P
Formatted: Font: Italic
Deleted: 7

and scaled hummock-hollow subplot NP_{pot} models.

To upscale models or plot-scale measurements it is important to determine the microtopographic structure and variability of a peatland. There were often non-bimodal distributions of microtopography in our study sites (Figures 3–4 A-panels and Table 2) where the more continuous distribution of elevation at the plot scale suggests that when experimental designs use hummock-hollow pairs as the primary experimental unit (Figures 3–4 B-panels) they have a tendency to capture the ends of the distribution, omitting on average 25% of the elevation distribution at the plot scale (see also Figure S6). In this study, we clipped vegetation in 50 small random plots to produce very high resolution DEMs for assessing microtope-scale (*i.e.* S3 hummock-hollow complex, *cf*. Belyea and Baird, 2006) variability, yet surface vegetation removal will generally be undesirable. Ground- or drone-based SfM approaches have been used to produce a digital surface model (DSM – vegetation present) for alpine (Mercer and Westbrook, 2016) and blanket (Harris and Baird, 2018) peatlands with reasonable accuracy (*e.g.* mean absolute error of ~0.08 m, and normalized median absolute deviation of ~0.11 m for the alpine and blanket peatlands, respectively). In situations where surface vegetation removal is not possible or desirable and/or where drone-based imagery is hampered (*e.g.* treed peatlands), a survey of height distribution along one or several transects would provide an alternative to assessing microtope to mesotope-scale (S3–S4 Belyea and Baird, 2006) microtopographic variability. The power spectral density of transect data would suggest that, for absolute height, a sampling interval of less than 1 m (*e.g.* 0.5 m) would capture the scales of variability which contribute most to total

Deleted: P

Deleted: .

Deleted: .

Deleted: 3

Formatted: Font: Italic

Deleted: for several 50 m transects

height variance (Figures 2 and 5) since this corresponds to ~95% of measured microtopographic variation and provide sufficient fine-scale data to estimate the fractal dimension of microtopography. Information on height distributions could provide the basis for plot selection, where plots could be chosen to deliberately span the range of variability, or to avoid oversampling extremes. Information on the height distribution would furthermore provide the ability to scale up findings from the plot level given their relative position in the wider distribution of microtopographic variability (*cf. Griffis* et al., 2000).

Deleted: .

Deleted: 90

Despite the variety of site characteristics observed, our plots were limited to bogs and poor fens, and did not include sites with ridge and pool patterning. Nevertheless, our results would suggest that generalizations based on a hummock-hollow classification, either to the site-scale, or to hummocks-hollow pairs across sites should be viewed with a degree of skepticism when sample size is low, or when a general microtopographic survey is absent/unreported. Thus, for wider inter-comparability of peatland studies, SfM or transect-based approaches of measuring and reporting on one or several morphometric properties of microtopography could provide a more comprehensive dataset to aid in future meta-analysis/synthesis.

Implications for appropriate complexity ecosystem modelling in peatlands

The complex shape/structure of peatland microtopography has generally been ignored from a modelling standpoint, but several studies have shown, for example, that slope and aspect may affect peat temperature (Kettridge and Baird 2010). Under clear-sky

conditions, modelled annual total solar insolation differs from a flat surface by roughly ±20% in our measured plots, where our study sites span 43° to 60°N latitude (Figure S10). For north and south facing slopes, this effect is amplified (Figure 7) particularly for high- and low-hummock microtopographic classes (*e.g.* Figure S4), which tend to have greater average slope compared to the hollow/lawn classification (Figure S9). While our study sites are limited to the non-permafrost boreal region, the applicability of slope and aspect considerations to modelling tundra tussocks in arctic and permafrost regions is also relevant (*e.g.* De Baets et al., 2016). Based on the results of empirical studies, the shape of microtopographic features ought to play a role in ecosystem fluxes due to the effect of shortwave radiation on surface evaporation (Kettridge and Baird, 2010), photosynthetically active radiation on moss production (Harley et al., 1989; Loisel et al., 2012), and soil temperature on methane production and respiration (*e.g.* Lafleur et al., 2005; Waddington et al., 2009). It is important to note, however, that under cloudy conditions the increasing proportion of total insolation from diffuse radiation decreases the disparity in insolation associated with slope and aspect. Furthermore, in peatlands where substantial tree, shrub, or graminoid cover exists, the importance of slope and aspect on soil heating or ecosystem fluxes is likely to be low since insolation decreases exponentially with increasing vascular leaf area.

In addition to microtopographic shape/structure, the size of microtopographic features and their small-scale variability can similarly affect ecosystem fluxes, where height above water table imposes a first order control on water availability. Methane fluxes from peatlands, for example, have been shown to vary logarithmically over 0.1 m scales

Deleted: 6

Formatted: Font: Italic

Deleted: S1

Deleted: S5

Deleted: a

(Turetsky et al., 2014). Water availability at the moss surface has been shown to be both species-dependent and strongly affected by water table (Hayward and Clymo, 1982; Rydin, 1985), where moss species and water availability has been linked to many ecohydrological processes such as surface evaporation (Kettridge and Waddington, 2014), productivity (Williams and Flanagan, 1998; Strack and Price, 2009), and hydrophobicity (Moore et al., 2017). We show that when microtopographic variability is explicitly modelled, complex patterns of potential moss productivity emerge (Figure S12) which are not necessarily captured by a hummock-hollow model (Figure 9), and that the presence of bias is independent of whether moss species niche partitioning is considered.

The SfM method is a potentially useful tool for examining how morphometric properties of the surface which affect ecohydrological processes vary within a site. Moreover, information on microtopographic variability from SfM-derived DEMs can be used to further examine the potential role of fine-scale microtopographic variability on biogeochemical processes within a modelling domain. The GMM is a simple way to include a more realistic description of height distributions within distributed peatland models (*e.g*. Dimitrov et al., 2010), or extend from the meso- to micro-scale (Sonnentag et al., 2008). Computationally, GMMs are a relatively efficient way of representing microtopographic variability, needing only two parameters per member of the GMM distribution. Conceptually, the GMM distribution can be applied directly in distributed peatland models to populate relative heights of individual cells. In the case of one-dimensional models, a GMM distribution can be used as a transfer function for any

Deleted: S8

Deleted: both

Deleted: and structure

water table-dependent processes, particularly in cases where the relation is non-linear. Alternatively, a small number of parameters from the PSD of microtopographic elevation (*e.g.* variance, Hurst exponent, and spatial scale of break point), be it from a transect (Figure 2) or DEM (Figure 5), can be used to generate 'synthetic' microtopography which includes spatial structure in elevation change rather than just the distribution.

Deleted:

Deleted: DEM (Fig. S4) or

Deleted: .

Deleted: .

CONCLUSIONS

The magnitude of variation in assessed morphometric properties within a site (randomly chosen plots) is commensurate with the range across sites (qualitative plots), where mean differences are comparatively small. With a small effect size, our results highlight the need for adequate spatial sampling in process-based studies of microform function, particularly when upscaling to the whole peatland or in order to make broader inferences regarding peatland microforms in general. The SfM technique provides very high resolution and accurate DEMs relatively quickly and easily. For studies which focus on processes which are correlated with microtopographic position, a DEM or DSM derived from ground- or drone-based imagery provides valuable information on microtopographic variability and structure which can help inform plot selection, be used for upscaling results, and quantify well defined morphometric and topographic variables to aid in study inter-comparisons. Conversely, height measurements (*e.g.* using a dGPS or other survey method) along a transect of at least 100 m with measurements taken at an interval of less than 1 m provides sufficient information to describe a number of peatland morphometric properties (*e.g.* hypsometry, roughness, fractal dimension, etc.).

Our study highlights the need to critically assess sampling approaches in peatland ecosystem science, where we show that a strict hummock-hollow classification tends to under-sample intermediate topographic positions. While the discretization of peatland ecosystems into microtopographic units has facilitated the understanding of peatland processes in the context of species niche partitioning and their covariates such as water table position, we now have techniques to better quantify variability with relative ease. Consequently, techniques such as SfM enable us to consider peatland ecosystem processes as part of a continuum. We must recognize that our conceptualizations, while perhaps representing necessary simplifications, ought to be scrutinized to ensure that elements of peatland complexity are not omitted. By considering microtopography explicitly, we may be better able to understand how ecosystem complexity subsumed within current microtopographic classifications might represent an important unquantified confounding variable which limits our ability to adequately resolve and thus understand certain peatland processes.

CODE/DATA AVAILABILITY

All data necessary to reproduce the results in the paper are available via 10.5281/zenodo.2545674. The data set also includes the script used to carry out all final analysis and figure production. Raw imagery or point clouds can be obtained by contacting the corresponding author directly.

Deleted: The post-processed point clouds used to generate digital elevation models which were analysed in this study are available online at: [File are currently uploaded to a project folder on Zenodo. Final publishing and assignment of DOI will be completed after review, where additional material may be added based on recommendation(s) from reviewers].

AUTHOR CONTRIBUTIONS

PAM, JMW, DKT, NK, and GG designed the study. All co-authors contributed to in situ data collection. Data post-processing and analysis was primarily done by PAM. PAM prepared the manuscript, with substantive editing and comments from all other co-authors.

COMPETING INTERESTS

The authors declare that they have no conflict of interest.

ACKNOWLEDGEMENTS

We would like to thank James Sherwood and Paul Morris for valuable conversations regarding the feasibility of this study and early discussions regarding research design. We thank Lorna Harris for comments on an earlier draft of this manuscript. We also thank Tom Ulanowski for data collection for the James Bay site, Rebekah Ingram and Kristyn Mayner for data collection at the Red Earth Creek site, Mandy MacDougall, Alanna Smolarz and Alex Furukawa for assistance with the Nobel data collection and analysis, and to Lee Slater for data collection in Maine. This research was supported by a NSERC Discovery Grant and NSERC Discovery Accelerator Supplement to JMW.

805 **REFERENCES**

806 Andrus, R., Wagner, D., and Titus, J.: Vertical zonation of *Sphagnum* mosses along
807 hummock-hollow gradients, Can. J. Bot., 61, 3128-3139, doi:10.1139/b83-352, 1983.

808 Belyea, L. R., and Baird, A. J.: Beyond "the limits to peat bog growth'": Cross-scale
809 feedback in peatland development, Ecol.l Monogr., 76, 299–322, doi: 10.1890/0012-
810 9615(2006)076[0299:BTLTPB]2.0.CO;2,2006.

811 Belyea, L. R., and Clymo, R. S.: Do hollows control the rate of peat bog growth.
812 *Patterned mires and mire pools*, 55-65, 1998.

813 Belyea, L. R., and Clymo, R. S.: Feedback control of the rate of peat formation. Proc. of
814 the Royal Soc. London B: Biol. Sci., 268, 1315-1321, doi:10.1098/rspb.2001.1665,
815 2001.

816 Belyea, L. R., and Malmer, N.: Carbon sequestration in peatland: Patterns and
817 mechanisms of response to climate change, Glob. Chang. Biol. 10, 1043–1052,
818 doi.org/10.1111/j.1529-8817.2003.00783.x, 2004.

819 Benscoter, B. W., Wieder, R. K., and Vitt, D. H.: Linking microtopography with post-fire
820 succession in bogs, J. Veg. Sci., 16, 453–460, doi:10.1111/j.1654-
821 1103.2005.tb02385.x, 2005.

822 Blodau, C., Basiliko, N., and Moore, T. R.: Carbon turnover in peatland mesocosms
823 exposed to different water table levels, Biogeochem., 67, 331-351,
824 doi:10.1023/B:BIOG.0000015788.30164.e2, 2004.

825 Brown, M., and Lowe, D. G.: Unsupervised 3D object recognition and reconstruction in

826 unordered datasets. Fifth International Conference on 3-D Digital Imaging and
827 Modeling, 56-63, doi:10.1109/3DIM.2005.81, 2005.

828 Bruland, G. L, and Richardson, C. J.: Hydrologic, edaphic, and vegetative responses to
829 microtopographic reestablishment in a restored wetland, Rest. Ecol., 13, 515-523,
830 doi:10.1111/j.1526-100X.2005.00064.x, 2005.

831 Bubier, J. L., Moore, T. R., and Roulet, N. T.: Methane emissions from wetlands in the
832 midboreal region of Northern Ontario, Canada, Ecol., 74, 2240-2254, doi:
833 10.2307/1939577, 1993.

834 Campbell, D. R., Duthie, H. C., and Warner, B. G.: Post-glacial development of a kettle-
835 hole peatland in southern Ontario, Ecosci., 4, 404-418,
836 doi:10.1080/11956860.1997.11682419, 1997.

837 Cresto Aleina F., Runkle B. R. K., Kleinen T., Kutzbach L., Schneider J., Brovkin V.:
838 Modeling micro-topographic controls on boreal peatland hydrology and methane
839 fluxes, Biogeosci., 12, 5689-5704, doi: 10.5194/bg-12-5689-2015, 2015.

840 Crill, P. M., Bartlett, K. B., Harriss, R. C., Gorham, E., Verry, E. S., Sebacher, D. I.,
841 Madzar, L., and Sanner, W.: Methane flux from Minnesota peatlands, Global
842 Biogeochem. Cycles, 2, 371-384, doi:10.1029/GB002i004p00371, 1988.

843 De Baets, S., van de Weg, M. J., Lewis, R., Steinberg, N., Meersmans, J., Quine, T. A.,
844 Shaver, G. R., and Hartley, I. P.: Investigating the controls on soil organic matter
845 decomposition in tussock tundra soil and permafrost after fire, Soil Biol. Biochem., 99,
846 108-116, doi: 10.1016/j.soilbio.2016.04.020, 2016.

Deleted: 2007

Deleted: ences

849 Dimitrov, D. D., Grant, R. F., Lafleur, P. M., and Humphreys, E. R.: Modeling peat
850 thermal regime of an ombrotrophic peatland with hummock–hollow microtopography,
851 Soil Sci. Soc. Am. J., 74, 1406-1425, doi:10.2136/sssaj2009.0288, 2010.

852 Eppinga, M., Rietkerk, M., Borren, W., Lapshina, E. D., Bleuten, W., and Wassen, M. J.:
853 Regular surface patterning of peatlands: Confronting theory with field data,
854 *Ecosystems*, 11, 520–536, doi:10.1007/s10021-008-9138-z, 2008.

855 Forbrich, I., Kutzbach, L., Wille, C., Becker, T., Wu, J., and Wilmking, M.: Cross-
856 evaluation of measurements of peatland methane emissions on microform and
857 ecosystem scale using high-resolution landcover classification and source weight
858 modelling, Ag. For. Met., 151, 864-874, doi:10.1016/j.agrformet.2011.02.006, 2011.

859 Frenzel. P, and Karofeld, E.: CH_4 emission from a hollow-ridge complex in a raised bog:
860 The role of CH_4 production and oxidation, Biogeochem., 51, 91-112,
861 doi:10.1023/A:1006351118347, 2000.

862 Granath, G., Wiedermann, M. M., and Strengbom, J.: Physiological responses to
863 nitrogen and sulphur addition and raised temperature in *Sphagnum balticum*,
864 Oecologia, 161, 481-490, doi:10.1007/s00442-009-1406-x, 2009.

865 Griffis, T. J., Rouse, W. R., and Waddington, J. M.: Scaling net ecosystem exchange
866 from the community to the landscape level at a subarctic fen, Glob. Change Biol., 6,
867 459-473, doi: 10.1046/j.1365-2486.2000.00330.x, 2000.

868 Harley, P. C., Tenhunen, J. D., Murray, K. J., and Beyers, J.: Irradiance and
869 temperature effects on photosynthesis of tussock tundra Sphagnum mosses from the

foothills of the Philip Smith Mountains, Alaska, Oecologia, 79(2), 251-259, doi: 10.1007/BF00388485, 1989.

Harris, A., and Baird, A. J., Microtopographic Drivers of Vegetation Patterning in Blanket Peatlands Recovering from Erosion, Ecosystems, 1-20, doi: 10.1007/s10021-018-0321-6, 2018.

Hayward, P. M., and Clymo, R. S.: Profiles of water content and pore size in Sphagnum and peat, and their relation to peat bog ecology. Proceedings of the Royal Society of London. Series B. Biological Sciences, 215(1200), 299-325, 1982.

Hodgkins, S. B., Richardson, C. J., Dommain, R., Wang, H., Glaser, P. H., Verbeke, B., Winkler, R. B., Cobb, A. R., Rich, V. I., Missilmani, M., Flanagan, N., Ho, M., Hoyt, A. M., Harvey, C. F., Vining, S. R., Hough, M. A., Moore, T. R., Richard, P. J. H., De La Cruz, F. B., Toufaily, J., Hamdan, R., Cooper, W. T., and Chanton, J. P.: Tropical peatland carbon storage linked to global latitudinal trends in peat recalcitrance. Nature Comm., 9, 3640, doi: 10.1038/s41467-018-06050-2, 2018.

Humphreys, E. R., Lafleur, P. M., Flanagan, L. B., Hedstrom, N., Syed, K. H., Glenn, A. J., and Granger, R.: Summer carbon dioxide and water vapor fluxes across a range of northern peatlands, J. Geophys. Res., 111, G04011, doi:10.1029/2005JG000111, 2006.

Ise, T., Dunn, A. L., Wofsy, S. C., and Moorcroft, P. R.: High sensitivity of peat decomposition to climate change through water-table feedback, Nature Geosci., 1, 763-766, doi:10.1038/ngeo331, 2008.

Kettridge, N., and Baird, A. J.: Modelling soil temperatures in northern peatlands, Eur. J. Soil Sci., 59, 327–338, doi:2389.2007.01000.x, 2008.

Kettridge, N., and Baird, A.: Simulating the thermal behavior of northern peatlands with a 3‐D microtopography, J. Geophys. Res.: Biogeosciences, 115, G03009, doi: 10.1029/2009JG001068, 2010.

Kettridge, N., and Waddington, J.M.: Towards quantifying the negative feedback regulation of peatland evaporation to drought, Hydrological Processes, 28(11), 3728-3740, doi: 10.1002/hyp.9898, 2014.

Kettridge, N., Comas, X., Baird, A., Slater, L., Strack, M., Thompson, D., Jol, H., and Binley, A.: Ecohydrologically important subsurface structures in peatlands revealed by ground-penetrating radar and complex conductivity surveys, J. Geophys. Res., 113, G04030, doi:10.1029/2008JG000787, 2008.

Kettridge, N., Turetsky, M. R., Sherwood, J. H., Thompson, D. K., Miller, C. A., Benscoter, B. W., and Waddington, J. M.: Moderate drop in water table increases peatland vulnerability to post-fire regime shift, Sci. Rep., 5, 8063, doi:10.1038/srep08063, 2015.

Kumar, L., Skidmore, A. K. and Knowles, E.: Modelling topographic variation in solar radiation in a GIS environment. International Journal of Geographical Information Science, 11(5), 475-497, doi: 10.1080/136588197242266, 1997.

Lafleur, P. M., Roulet, N. T., Bubier, J. L., Frolking, S., and Moore, T. R.: Interannual variability in the peatland-atmosphere carbon dioxide exchange at an ombrotrophic

bog. Glob. Biogeochem. Cycles, 17, 1036, doi:10.1029/2002GB001983, 2003.

Lafleur, P. M., Moore, T. R., Roulet, N. T., and Frolking, S.: Ecosystem respiration in a cool temperate bog depends on peat temperature but not water table, Ecosystems, 8, 619-629, doi:10.1007/s10021-003-0131-2, 2005.

Laing, C. G., Shreeve, T. G., and Pearce, D. M. E.: Methane bubbles in surface peat cores: in situ measurements, Glob. Change Biol., 14, 916–924, doi:10.1111/j.1365-2486.2007.01534, 2008.

Larsen, L. G., Eppinga, M. B., Passalacqua, P., Getz, W. M., Rose, K. M. and Liang, M.: Appropriate complexity landscape modeling, Earth Sci. Rev., 160, 111-130, doi:10.1029/2008JG000787, 2016.

Loisel, J., Gallego-Sala, A. V., and Yu, Z. C.: Global-scale pattern of peatland Sphagnum growth driven by photosynthetically active radiation and growing season length, Biogeosciences, 9, 2737-2746, doi: 10.5194/bg-9-2737-2012, 2012.

Lowe, D. G.: Object recognition from local scale-invariant features. The proceedings of the seventh IEEE international conference on Computer vision, 2, 1150-1157, doi:10.1109/ICCV.1999.790410, 1999.

Lukenbach, M. C., Kettridge, N., Devito, K. J., Petrone, R. M., and Waddington, J. M.: Hydrogeological controls on post-fire moss recovery in peatlands, J. Hydrol., 530, 405-418, doi:10.1016/j.jhydrol.2015.09.075, 2015.

Maholtra, A., Roulet, N. T., Wilson, P., Giroux-Bougard, X., and Harris, L. I.: Ecohydrological feedbacks in peatlands: an empirical test of the relationship among

vegetation, microtopography and water table, Ecohydrol., 9, 1346-1357, doi:1002/eco.1731, 2016.

MathWorks, Inc.: MATLAB, Version 8.5, MathWorks, Natick, Mass., 2015.

Mercer, J. J., and Westbrook, C. J.: Ultrahigh-resolution mapping of peatland microform using ground-based structure from motion with multiview stereo, J. Geophys. Res. Biogeosci., 121, 2901-2916, doi:10.1002/2016JG003478, 2016.

Moore, T. R.: Growth and net production of Sphagnum at five fen sites, subarctic eastern Canada. Canadian Journal of Botany, 67(4), 1203-1207, doi: 10.1139/b89-156, 1989.

Moore, T. R., and Roulet, N. T., and Waddington, J. M.: Uncertainty in predicting the effect of climatic change on the carbon cycling of Canadian peatlands, Clim. Change, 40, 229-245, doi:10.1023/A:1005408719297, 1998.

Moore, P. A., Morris, P. J., and Waddington, J. M.: Multi-decadal water table manipulation alters peatland hydraulic structure and moisture retention, Hydrol. Proc., 29, 2970-2982, doi:10.1002/hyp.10416, 2015.

Moore, P. A., Lukenbach, M. C., Kettridge, N., Petrone, R. M., Devito, K. J. and Waddington, J. M.: Peatland water repellency: Importance of soil water content, moss species, and burn severity, Journal of Hydrology, 554, 656-665, doi: 10.1016/j.jhydrol.2017.09.036, 2017.

Moore, P. A., Smolarz, A. G., Markle, C. E., and Waddington, J. M.: Hydrological and thermal properties of moss and lichen species on rock barrens: Implications for

954 turtle nesting habitat, Ecohydrol., 12, e2057, doi:10.1002/eco.2057, 2019.

955 Moser, K., Ahn, C., and Noe, G.: Characterization of microtopography and its influence
956 on vegetation patterns in created wetlands, Wetlands, 27, 1081-1097, doi:
957 10.1672/0277-5212(2007)27[1081:COMAII]2.0.CO;2, 2007.

958 Nijp, J. J., Limpens, J., Sjoerd, K. M., van der Zee, E. A. T. M., Berendse, F., and
959 Robroek, B. J. M.: Can frequent precipitation moderate the impact of drought on
960 peatmoss carbon uptake in northern peatlands? New Phytol., 203, 70-80,
961 doi:10.1111/nph.12792, 2014.

962 Nungesser, M. K.: Modelling microtopography in boreal peatlands: hummocks and
963 hollows, Ecol. Mod., 165, 175-207, doi:10.1016/S0304-3800(03)00067-X, 2003.

964 Pedrotti, E., Rydin, H., Ingmar, T., Hytteborn, H., Turunen, P., and Granath, G.:
965 Fine-scale dynamics and community stability in boreal peatlands: revisiting a
966 fen and a bog in Sweden after 50 years, Ecosphere, 5, 133, doi: 10.1890/ES14-
967 00202.1, 2014.

968 Peichl, M., Öquist, M., Löfvenius, M.O., Ilstedt, U., Sagerfors, J., Grelle, A., Lindroth, A.,
969 and Nilsson, M.B.: A 12-year record reveals pre-growing season temperature and
970 water table level threshold effects on the net carbon dioxide exchange in a boreal fen,
971 Env. Res. Lett., 9, 055006, doi: 10.1088/1748-9326/9/5/055006, 2014.

972 Pelletier, L., Garneau, M., and Moore, T. R.: Variation in CO_2 exchange over three
973 summers at microform scale in a boreal bog, Eastmain region, Québec, Canada, J.
974 Geophys. Res., 116, G03019, doi:10.1029/2011JG001657, 2011.

975 Petrone, R. M., Solondz, D. S., Macrae, M. L., Gignac, D., and Devito, K. J.:
976 Microtopographical and canopy cover controls on moss carbon dioxide exchange in a
977 western Boreal Plain peatland. Ecohydrol., 4, 115-129, doi:10.1002/eco.139, 2011.

978 Rahman, M. M., McDermid, G. J., Strack, M., and Lovitt, J.: A new method to map
979 groundwater table in peatlands using unmanned aerial vehicles, Rem. Sens., 9,
980 1057, doi: 10.3390/rs9101057 , 2017.

981 Regina, K., Nykänen, H., Silvola, J., and Martikainen, P. J.: Fluxes of nitrous oxide from
982 boreal peatlands as affected by peatland type, water table level and nitrification
983 capacity, Biogeochem., 35, 401-418, doi:10.1007/BF02183033, 1996.

984 Robroek, B. J., Schouten, M. G., Limpens, J., Berendse, F. and Poorter, H.: Interactive
985 effects of water table and precipitation on net CO2 assimilation of three co‐
986 occurring Sphagnum mosses differing in distribution above the water table, Global
987 Change Biology, 15(3), 680-691, doi: 10.1111/j.1365-2486.2008.01724.x,2009.

988 Rydin, H.: Effect of water level on desiccation of *Sphagnum* in relation to surrounding
989 Sphagna, Oikos, 45(3), 374-379, doi: 10.2307/3565573, 1985.

990 Rydin, H., and Mcdonald, A. J. S.: Tolerance of *Sphagnum* to water level, J. Bryol., 13,
991 571-578, doi:10.1179/jbr.1985.13.4.571.,1985.

992 Shannon, R. D., and White, J. R.: A three-year study of controls on methane emissions
993 from two Michigan peatlands, Biogeochem., 27, 35-60, doi:10.1007/BF00002570,
994 1994.

995 Sonnentag, O., Chen, J. M., Roulet, R. T., Ju, W., and Govind, A.: Spatially explicit

simulation of peatland hydrology and carbon dioxide exchange: Influence of mesoscale topography, J. Geophys. Res., 113, G02005, doi:10.1029/2007JG000605, 2008.

Strack, M., and Price, J.S.: Moisture controls on carbon dioxide dynamics of peat - *Sphagnum* monoliths. Ecohydrology, 2(1), 34-41, doi: 10.1002/eco.36, 2009

Turetsky, M., Wieder, K., Halsey, L., and Vitt, D.: Current disturbance and the diminishing peatland carbon sink, Geophys. Res. Lett., 29, 1526, doi:10.1029/2001GL014000, 2002.

Turetsky, M. R., Kotowska, A., Bubier, J., Dise, N. B., Crill, P., Hornibrook, E. R. C., Minkkinen, K., Moore, T. R., Myers-Smith, I. H., Nykänen, H., Olefeldt, D., Rinne, J., Saarnio, S., Shurpali, N., Tuittila, E-S., Waddington, J. M., White, J. R., Wickland, K. P., and Wilmking, M.: A synthesis of methane emissions from 71 northern, temperate, and subtropical wetlands, Glob. Change Biol., 20, 2183-2197, doi:10.1111/gcb.12580, 2014.

Ulanowski, T. A., and Branfireun, B. A.: Small-scale variability in peatland pore-water biogeochemistry, Hudson Bay Lowland, Canada, Sci. Tot, Environ., 454-455, 211-218, doi:10.1016/j.scitotenv.2013.02.087, 2013.

Waddington, J. M., and Roulet, N. T.: Atmosphere-wetland carbon exchanges: Scale dependency of CO_2 and CH_4 exchange on the developmental topography of a peatland, Global Biogeochem. Cycles, 10, 233-245, doi:10.1029/95GB03871, 1996.

Waddington, J. M., Rochefort, L. and Campeau, S.: Sphagnum production and

1017 decomposition in a restored cutover peatland. Wetlands Ecology and Management,
1018 11, 85-95, doi: 10.1023/A:1022009621693, 2003.

1019 Waddington, J. M., Harrison, K., Kellner, E., and Baird, A. J.: Effect of atmospheric
1020 pressure and temperature on entrapped gas content in peat, Hydrol. Proc., 23, 2970-
1021 2980, doi: 10.1002/hyp.7412, 2009.

1022 Waddington, J. M., Morris, P. J., Kettridge, N., Granath, G., Thompson, D. K., and
1023 Moore, P. A.: Hydrological feedbacks in northern peatlands, Ecohydrology, 8, 113-
1024 127, doi:10.1002/eco.1493, 2015.

1025 Wieder, R. K., Scott, K. D., Kamminga, K, Vile, M. A., Vitt, D. H., Bone, T., Xu, B. I.,
1026 Benscoter, B. W., and Bhatti, J. S.: Postfire carbon balance in boreal bogs of Alberta,
1027 Canada, Glob. Change Biol., 15, 63-81, doi:10.1111/j.1365-2486.2008.01756.x, 2009.

1028 Williams, T. G., and Flanagan, L. B.: Measuring and modelling environmental influences
1029 on photosynthetic gas exchange in Sphagnum and Pleurozium. Plant, Cell &
1030 Environment, 21(6), 555-564, doi: 10.1046/j.1365-3040.1998.00292.x,1998.

1031 Wu, C.: VisualSFM: A visual structure from motion system, 2011.

1032 Yu, Z. C.: Northern peatland carbon stocks and dynamics: a review, Biogeosci., 9,
1033 4071–4085, doi: 10.5194/bg-9-4071-2012, 2012.

1034 Yu, Z., Beilman, D. W., and Jones, M. C.: Sensitivity of northern peatland carbon
1035 dynamics to Holocene climate change, Carbon cycling in northern peatlands, pages
1036 55-69, doi:10.1029/2008GM000822, 2009.

Table 1: Summary information, including latitude (Lat.) and longitude (Lon.), on sample locations and SfM reconstructions of microtopographic variation for randomly and qualitatively chosen plots. Sites listed below correspond only to those for plot-level analyses.

Location	Plot Name	Lat.	Lon.	Plot Area (m^2)	Number of Images Used	Point Cloud Density (m^{-2})
Random						
Nobel, ON[1]	Alpha	45.434	-80.081	4.6	47	6.04×10^4
--	Beta	--	--	3.8	41	7.83×10^4
--	Gamma	--	--	4.1	44	6.68×10^4
--	Epsilon	--	--	5.2	53	8.38×10^4
--	Zeta	--	--	6.12	66	1.60×10^5
--	Eta	--	--	5.74	60	1.42×10^5
--	Iota	--	--	5.66	49	3.23×10^4
--	Kappa	--	--	5.53	66	1.77×10^5
--	Theta	--	--	5.48	59	1.38×10^5
Qualitative						
Caribou Bog, MN[2]	Maine	44.83	-68.75	10.1	79	3.75×10^4
James Bay, ON[3]	JamesBay	52.846	-83.930	7.6	82	1.97×10^5
Ottawa, ON	Limerick	44.877	-75.609	9.0	282	5.94×10^5
Puslinch, ON[4]	Puslinch	43.407	-80.264	6.45	109	1.12×10^5
Rödmossen, SWE[5]	Sweden	60.013	17.355	10.6	105	4.71×10^4
Seney, MI[6]	WET	46.190	-86.019	7.7	135	1.12×10^5
Seney, MI[6]	INT	46.192	-86.019	7.0	109	9.44×10^4
Seney, MI[6]	DRY	46.186	-86.015	7.3	62	8.89×10^4
Nobel, ON[1]	Lambda	45.434	-80.081	8.2	61	1.18×10^4

For detailed site information see the following studies: 1. Moore et al., (2019); 2. Kettridge et al. (2008); 3. Ulanowski and Branfireuen (2013); 4. Campbell et al. (1997); 5. Granath et al. (2009); 6. Moore et al. (2015).

Deleted: for target areas

Deleted: locations within a site

Deleted: (°N)

Deleted: (°W)

Deleted: --

Deleted: -

Table 2: Estimated parameters for one-, two-, or three-member Gaussian mixture model (GMM) fit to elevation distribution of plot-level digital elevation models, Results are presented for the GMM which minimizes AIC. Plots are separated into those chosen at random versus qualitatively at their respective site.

Deleted: DEM elevations

Location	Plot Name	1st distribution			2nd distribution			3rd distribution		
		Mean	SD	Scale	Mean	SD	Scale	Mean	SD	Scale
Random										
Nobel, ON	Alpha	0.11	0.03	0.23	0.20	0.03	0.36	0.28	0.06	0.41
--	Beta	0.13	0.04	0.37	0.18	0.03	0.53	0.29	0.04	0.10
--	Epsilon	0.07	0.02	0.06	0.18	0.05	0.30	0.31	0.05	0.64
--	Gamma	0.19	0.08	0.23	0.26	0.04	0.59	0.44	0.06	0.18
--	Zeta	0.11	0.03	1	—	—	—	—	—	—
--	Eta	0.13	0.04	0.82	0.25	0.05	0.18	—	—	—
--	Iota	0.11	0.03	0.24	0.19	0.06	0.76	—	—	—
--	Kappa	0.11	0.04	0.23	0.23	0.06	0.60	0.42	0.05	0.06
--	Theta	0.16	0.03	0.84	0.25	0.04	0.16	—	—	—
Qualitative										
Caribou Bog, ME	Maine	0.07	0.02	0.15	0.16	0.02	0.55	0.28	0.07	0.30
James Bay, ON	JamesBay	0.17	0.08	1	—	—	—	—	—	—
Ottawa, ON	Limerick	0.08	0.02	0.38	0.15	0.05	0.62			
Puslinch, ON	Puslinch	0.14	0.053	1	—	—	—	—	—	—
Rödmossen	Sweden	0.17	0.05	0.87	0.36	0.04	0.13	—	—	—
Seney, MI	WET	0.23	0.08	0.59	0.36	0.05	0.25	0.44	0.03	0.16
Seney, MI	INT	0.25	0.07	0.51	0.45	0.06	0.40	0.53	0.02	0.09
Seney, MI	DRY	0.08	0.03	0.05	0.21	0.04	0.45	0.34	0.05	0.50
Nobel, ON	Lambda	0.05	0.02	0.46	0.20	0.08	0.54	—	—	—

LIST OF FIGURES:

Figure 1: Site-level relation between standard deviation of microtopographic variation based on total sample area for the Red Earth Creek site based on fifty ~3.5 m^2 plots. The grey shaded area represents the 2.5 and 97.5 percentile of standard deviation from the Monte Carlo resampling procedure.

Deleted: R

Figure 2: Site-level absolute (solid lines) and cumulative (dashed lines) power spectral density of height along a 300 m transect for the Red Earth Creek, AB (red) and Nobel, ON (black) sites.

Deleted: A

Figure 3: Plot-level relative frequency distribution of height in plots where a perceived representative hummock and adjacent hollow was subjectively chosen for a given site (Table 1 – Qualitative plot locations). Relative height distributions are shown for the entire plot (A) and for a hummock and hollow subplot (B) whose area corresponds to the size of a large flux measurement chamber. Elevations are referenced to the lowest point of the reconstructed surface and set to zero.

Deleted: R

Figure 4: Plot-level relative frequency distribution of height in plots with randomly chosen locations within a site containing a perceived hummock and adjacent hollow (Table 1 – Random plot locations). Relative height distributions are shown for the entire plot (A) and for a hummock and hollow subplot (B) whose area corresponds to the size of a large flux measurement chamber. Elevations are referenced to the lowest point of the reconstructed surface and set to zero.

Deleted: R

Figure 5: Plot-level radially averaged power spectral density for randomly– (left panel) and qualitatively– (right panel) chosen plots (Table 1) representing the change in elevation variability with length scale. The slope between the power spectral density and wavelength in log-log space corresponds with the Hurst exponent (*H*), where slope = -2(*H*+1); and is related to the fractal dimension as 3-*H*.

Figure 6: Plot-level Weibull probability density function of slope derived from the surface normal of a planar fit to elevation in a moving 0.03 m x 0.03 m window for all DEMs. Panels (a) and (b) separate the randomly and qualitatively chosen plots, respectively.

Figure 7: Variation in potential solar insolation relative to a flat surface based on aspect (a) and slope (b). Boxplots shows median and inter-quartile range, with outliers shown as dots. Insolation as a function of slope has been bin averaged per cardinal direction, where each point represents 100 data points. Slope and aspect data are for the Seney, WET plot.

Figure 8: Plots-scale mean potential net photosynthesis (NP) for three microtopographic classes (i.e. high-hummock, low-hummock, and lawn/hollow — see supplementary figure 1) derived from spatially explicit elevation data for random (a,c) and qualitatively chosen (b,d) plots. NP-WC and WC-WTD relations are based on separate parameterization for each microtopography class (see Figure S5).

Deleted: R
Formatted: Justified
Deleted: wavevector
Deleted: (2×π/wavelength)
Deleted: M
Deleted: P
Deleted: P
Deleted: supplementary
Deleted: f
Deleted: S2

Figure 9: Difference in plot-scale potential net photosynthesis (NP_{pot}) between models using the measured distribution of elevation over the entire SfM-derived DEM and the measured distribution within hummock-hollow subplots. NP_{pot} is modelled using separate parameterization (see Figure S5) for each microtopography class (a), as well as a uniform (low-hummock) parameterization across microtopography classes (b).

Figure 10: Difference in plot-scale potential net photosynthesis (NP_{pot} – as a percentage of max) based on a coarse to fine discretization of elevation values (n_z = 2 to 30) (see Figure S13 for example). NP_{pot} is modelled using separate parameterizations (see Figure S5) for each microtopography class (a), as well as a uniform (low-hummock) parameterization across microtopography classes (b). RMSE was calculated using NP_{pot} from the original plot-level DEMs as the reference values. Discretized elevation values for each plot are based on elevation percentiles ($p_{z,i}$) where $p_{z,i} = (i-1)\frac{100}{n_z} + \frac{50}{n_z}$; for i=1 to n_z.

Deleted: maximum
Deleted: P
Deleted: P
Deleted: 2
Formatted: Subscript
Formatted: Font: Italic

1135 [Figure 1]

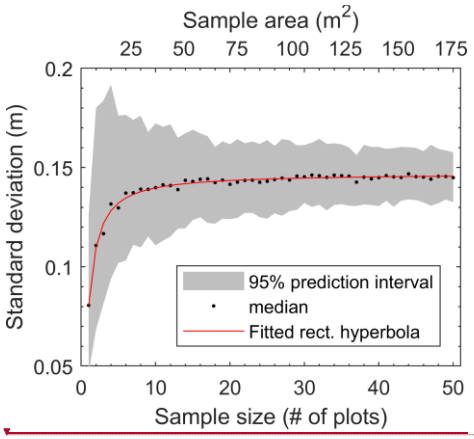

1136

1137

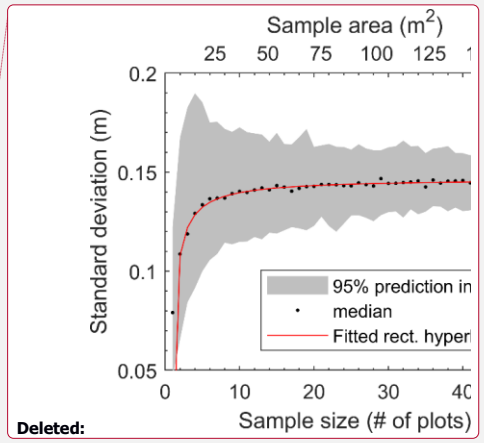

Deleted:

1139 [Figure 2]

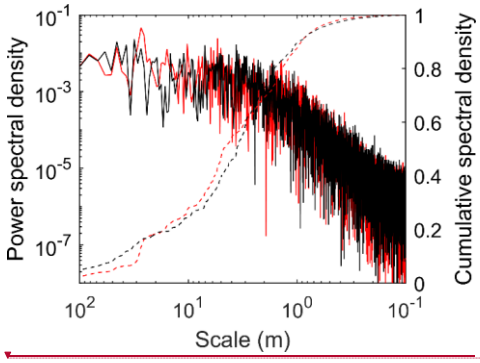

1140

1141

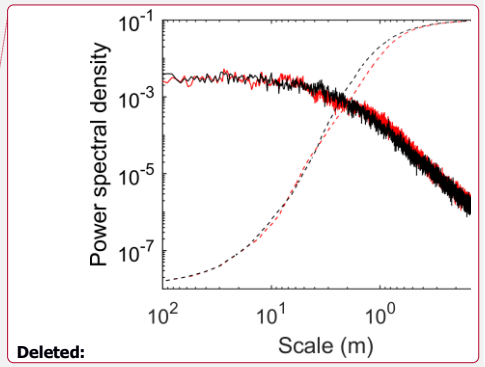

Deleted:

1143 [Figure 3]

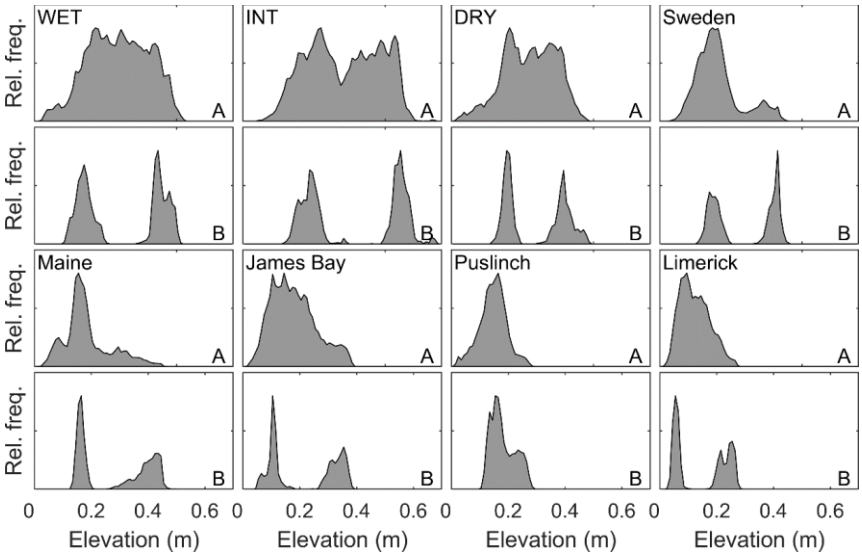

1144

1145

1146 [Figure 4]

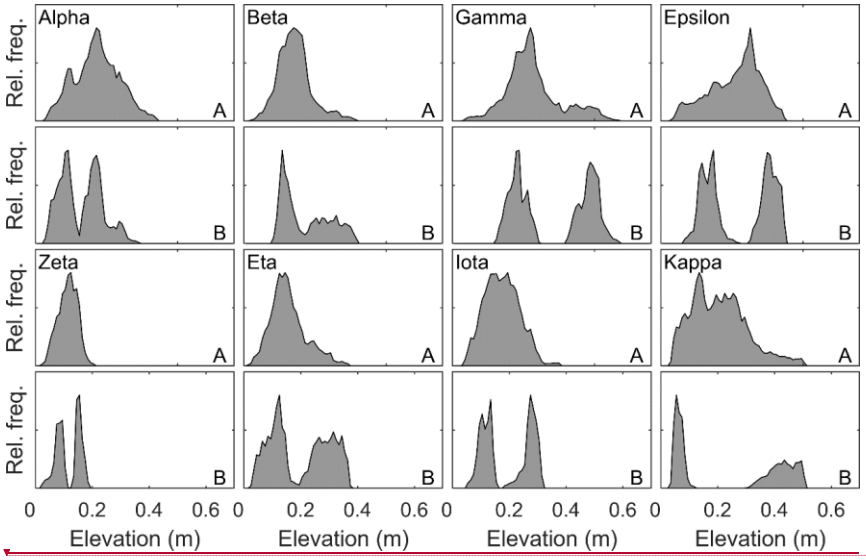

1147

1148

Deleted:

1150 [Figure 5]

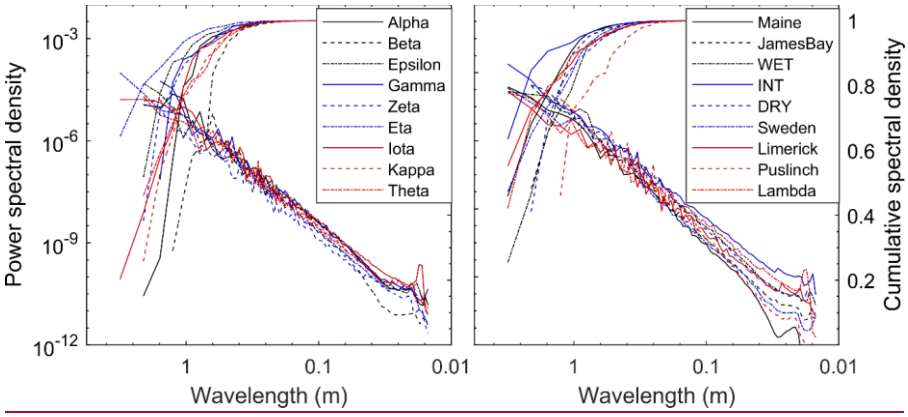

1151

1152

1153 [Figure 6]

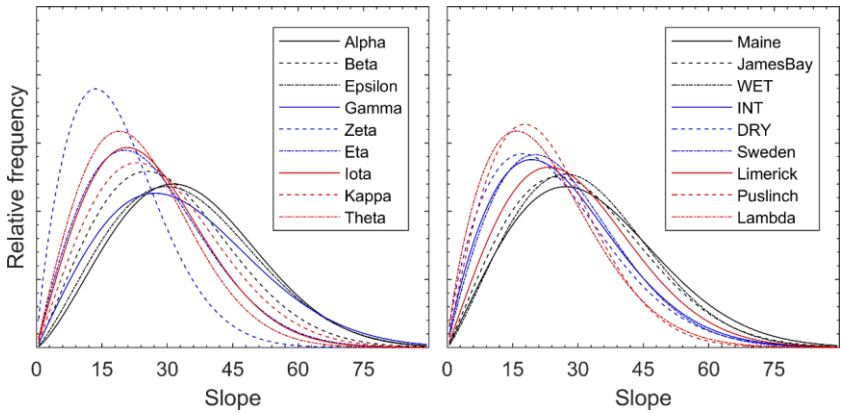

1154

1155

1156

1157 [Figure 7]

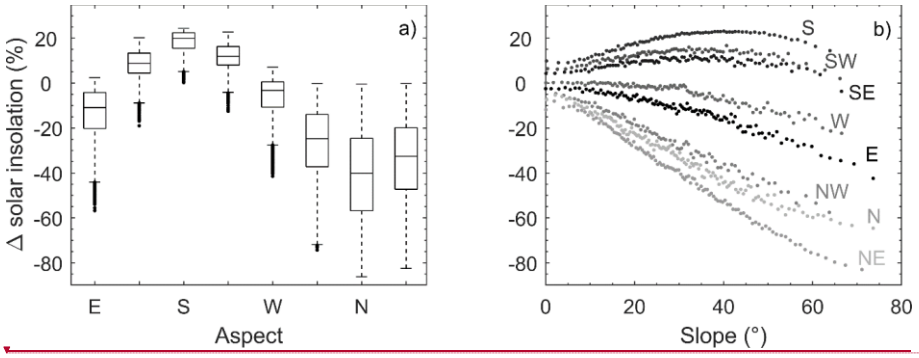

1158

1159

1160

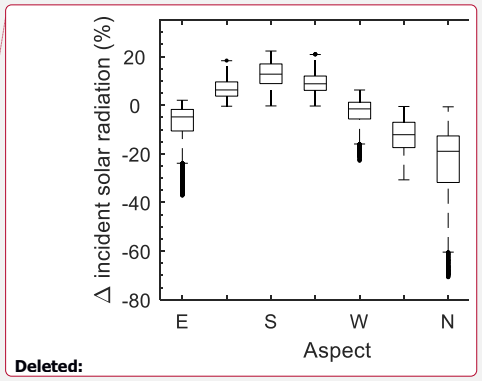

Deleted:

1162 [Figure 8]

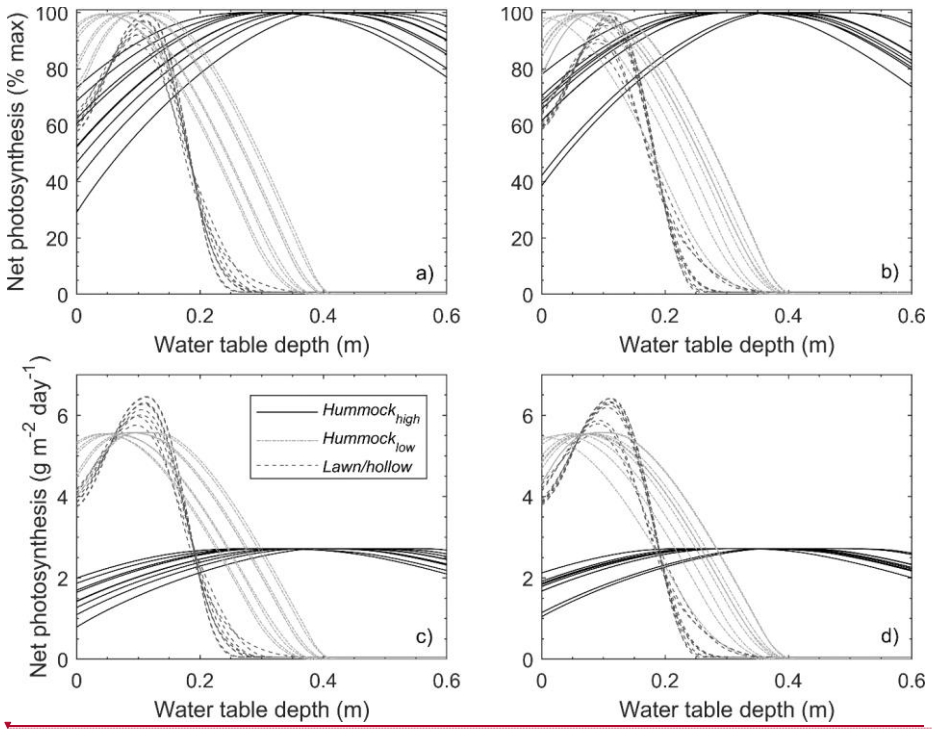

1163

1164

1165

Deleted:

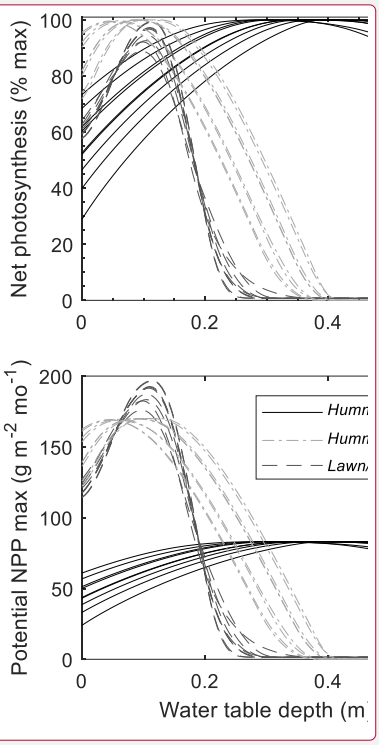

1167 [Figure 9]

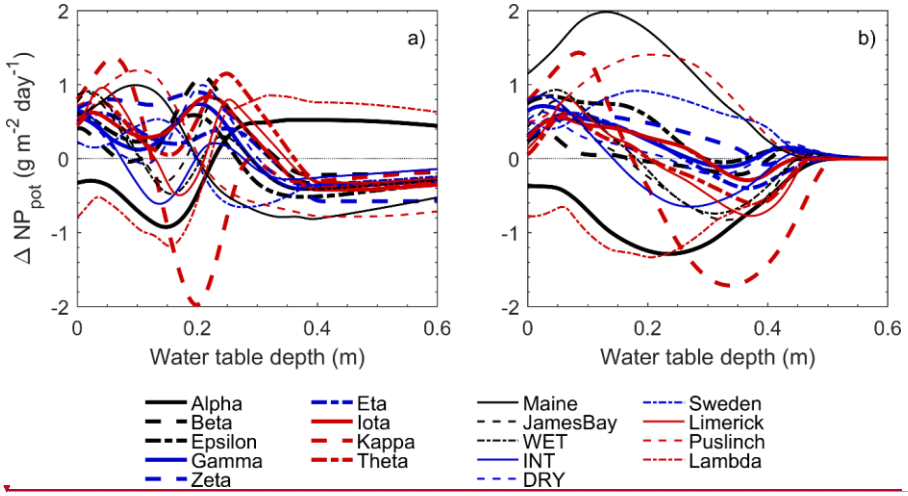

1168

1169

Deleted:

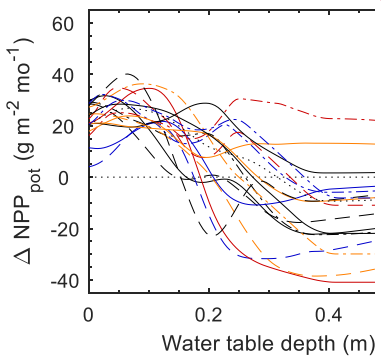

[Figure 10]

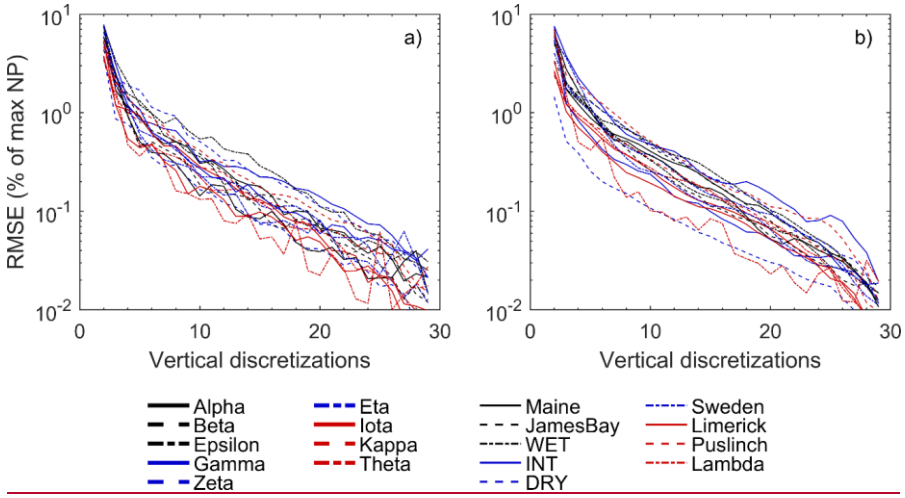
a)
b)
RMSE (% of max NP)
Vertical discretizations
Vertical discretizations
Alpha
Beta
Epsilon
Gamma
Zeta
Eta
Iota
Kappa
Theta
Maine
JamesBay
WET
INT
DRY
Sweden
Limerick
Puslinch
Lambda